Mathematical Model of Accumulation of Damaged Proteins and its Impact on Ageing

Dissertation

zur Erlangung
des Doktorgrades der Naturwissenschaften

eingereicht am
Fachbereichs Mathematik und Informatik
der Freien Universität Berlin

Vorgelegt von
Marija Cvijovic

Datum und Ort der mündlichen Prüfung: 30. Januar 2009 in Berlin

Gutachter:
Prof. Dr. Edda Klipp
Prof. Dr. Alexander Bockmayr
Prof. Dr. Per Sunnerhagen

Brain is like a parachute. It works best when it is open.

Frank Zappa

Abstract

Unlike most microorganisms or cell types, the yeast *Saccharomyces cerevisiae* undergoes asymmetrical cytokinesis, resulting in a large mother cell and a smaller daughter cell. The mother cells are characterized by a limited replicative potential accompanied by a progressive decline in functional capacities, including an increased generation time. Accumulation of oxidized proteins, a hallmark of ageing, has been shown to occur also during mother cell-specific ageing, starting during the first G1 phase of newborn cells. It has been shown that such oxidatively damaged proteins are inherited asymmetrically during yeast cytokinesis such that most damage is retained in the mother cell.

To investigate the potential benefits of asymmetrical cytokines, we created a mathematical model to simulate the robustness and fitness of dividing systems displaying different degrees of damage segregation and size asymmetries.

The model suggests that systems dividing asymmetrically (size-wise) or displaying damage segregation are more robust than fully symmetrical systems, i.e. can withstand higher degrees of damage before entering clonal senescence. Both size and damage asymmetries resulted in a separation of the population into a rejuvenating and an aging lineage. When considering population fitness, a system producing different-sized progeny, like budding yeast, is predicted to benefit from damage retention only at high damage propagation rates. In contrast, the fitness of a system of equal-sized progeny is enhanced by damage segregation regardless of damage propagation rates suggesting that damage partitioning may provide an evolutionary advantage also in systems dividing by binary fission. Using *S. pombe* as a model, we demonstrate experimentally that damaged, oxidized, proteins are unevenly partitioned during cytokinesis and that the damage-enriched sibling suffers from a prolonged generation time and an accelerated aging.

We demonstrate that the damage-enriched cell exhibits a reduced fitness and a shorter replicative life span. The model confirms the findings in budding yeast and moreover simulations suggest that asymmetrical distribution of damage increases the fitness of the cell population as a whole at both low and high damage propagation rates and pushes the upper limits for how much damage the system can endure before entering clonal

senescence. Thus, we suggest that “sibling-specific” aging in unicellular systems may have evolved as a byproduct of the strong selection for damage segregation during cytokinesis, and may be more common than previously anticipated.

Zusammenfassung

Im Gegensatz zu den meisten anderen Mikroorganismen oder Zelltypen teilt sich die Hefe *Saccharomyces cerevisiae* asymmetrisch in eine Mutter- und eine Tochterzelle. Das Potential zur Replikation ist bei den Mutterzellen limitiert und begleitet von einer graduellen Abnahme der funktionalen Kapazitäten, inklusive einer erhöhten Teilungsdauer. Die Ansammlung von oxidierten Proteinen, eines der Kennzeichen der Zellalterung, konnte bereits in früheren Studien in Mutterzellen während der Zellteilung nachgewiesen werden. Der Beginn dieses Prozesses liegt in der G1 - Phase des Zellzyklusses. In den früheren Arbeiten wurde auch gezeigt, dass die beschädigten Proteine während der Zellteilung asymmetrisch auf Mutter- und Tochterzelle aufgeteilt werden und der größte Schaden in der Mutterzelle verbleibt.

Im Rahmen dieser Arbeit wurde ein mathematisches Modell erstellt, mit welchem die potentiellen Vorteile asymmetrischer Zellteilung untersucht wurden. Der Fokus wurde dabei auf die Auswirkungen von unterschiedlicher Verteilung des oxidativen Schadens auf Mutter- und Tochterzelle sowie der Größenasymmetrie von Mutter und Tochter auf Fitness und Robustheit des Zellsystemes gelegt.

Die Resultate der Simulationen des Modelles deuten darauf hin, dass Zellsysteme mit asymmetrischer Teilung oder mit unterschiedlicher Verteilung des oxidativen Schadens robuster sind als Systeme mit symmetrischer Teilung. Asymmetrische Systeme akkumulieren beispielsweise einen größeren Schaden, bevor die klonale Seneszenz erreicht wird. Sowohl Größen- als auch Schadensasymmetrien führen zu einer Auftrennung der Population in eine sich verjüngende und eine alternde Zelllinie. Bei der Betrachtung der Fitness der Populationen zeigte sich, dass Systeme, die Nachkommen mit einer Größe verschiednen von den Elternzellen produzieren, wie das bei *S. Cerevisiae* der Fall ist, nur bei hohen Schadensprogationsraten vom Verbleib des Schadens in der Mutterzelle profitieren. Im Gegensatz dazu wird die Fitness von sich symmetrisch teilenden Systemen unabhängig von der Schadenspropagationsrate durch Aufteilung des Schadens erhöht. Dies deutet darauf hin, dass die Aufteilung des Schadens Systemen mit binärer Spaltung einen evolutionären Vorteil verschafft. Im Experiment konnte für *S.*

Pombe als Modelorganismus für ein solches System gezeigt werden, dass der oxidative Schaden während der Zellteilung in unterschiedlicher Höhe auf die Geschwisterzellen aufgeteilt werden. Die Zelle, bei der der höhere Schaden verbleibt, teilt sich in der Folge langsamer und altert schneller.

Es konnte ebenfalls gezeigt werden, dass die Fitness sowie die replikative Lebensspanne in Zellen mit höheren oxidativen Schäden reduziert ist. Das Model bestätigt die experimentellen Resultate für *S. Cerevisiae* und legt außerdem nahe, dass die asymmetrische Verteilung des Schadens die Fitness einer Zellpopulation sowohl für hohe als auch für niedrige Schadenspropagationsraten erhöht. Darüber hinaus wird dadurch die obere Schranke für den Schaden, ab welcher klonale Seneszenz erfolgt, weiter nach oben verlagert. Dies bedeutet, dass das geschwisterspezifische Altern als evolutionäres Nebenprodukt aus dem Selektionsvorteil für Systeme mit asymmetrischer Schadensaufteilung entstanden ist und möglicherweise weiter verbreitet ist, als bislang angenommen wurde.

Table of Contents

List of Figures

List of Tables

1. Systems Biology

The term *Systems Biology* appeared first time in 1966, when Mihajlo Mesarovic organized a "Systems Theory and Biology" symposium at Case Institute of Technology in Cleveland, Ohio. Even though more then 40 years past since that meeting, we consider that field of Systems Biology is still in its infancy.

The rapid progress in molecular biology of accurate, quantitative experimental approaches, high-throughput measurements, created a fruitful foundation for a new discipline. Yet, the identification of all components of the system doesn't give us an answer how the system works. Systems biology today combines the knowledge from various disciplines. Complementing biological reasoning, together with mathematics, physics, chemistry and computer science we are trying to resolve the complexity of biological systems.

A cell contains a countless numbers of molecules which interact in a very complex, sometimes in seemingly random fashion, and yet hold enough information to recreate another organism. Putting all the pieces together is like solving gigantic puzzle and represents one of the biggest scientific challenges of this century. It is likely that these pieces of the puzzle will never be easily understandable without the assistance of mathematical modeling.

Use of computational modeling has emerged as a powerful descriptive and predictive tool that allows the study of complex systems to investigate biological phenomena and is one of the most important techniques used in biology today. The role of mathematical modeling and simulations is to generate test hypothesis, design experiments and experimental data.
Hypotheses generated by *in silico* experiments are then tested by *in vivo* and *in vitro* studies.

1.1 Modeling Biological Systems

Biology is one of the most rapidly expanding and diverse areas in sciences. The problems encountered in biology are frequently complex and often not totally understood. Mathematical models provide means to better understand the processes and unravel some of the complexities.

The aim is to construct the model in the simplest possible way, but sill retaining the most important features of the system. The good model will be able to agree as closely as possible with the real world observations of the phenomenon we are trying to model and at the same time be interrogative.

Depending on the process we want to model, the available data and the goal we want to achieve, biological processes can be modeled using one of the following methods: Boolean Networks, Stochastic models or Ordinary Differential Equations.

1.1.1 Boolean Networks

The first Boolean networks were proposed by Stuart Kauffman in 1969, as random models of genetic regulatory networks.
The term *Boolean networks* refer to abstract mathematical models with large number of coupled variables. They are often use in understanding phenomena like genetic and metabolic networks, immune systems and neural networks.
In more formal way we can define a Boolean network as a set of nodes G corresponding to genes $V = \{x_1, \ldots, x_n\}$ and a list of Boolean functions $F = (f_1, \ldots, f_n)$. The state of a node (gene) is completely determined by the values of other nodes at time t by means of the underlying logical Boolean functions. The model is represented in the form of directed graph. In this approach each variable has two states: ON and OFF, more specifically, each x_i is the expression of a gene, with possible values 1 or 0, which give

either expressed or not expressed gene; while F represents the rules of the regulatory interactions between genes. In this way the system will deterministically go from one state to another. An advantage of this method is fast computation time, but a draw back is that variables are discrete and there is no precise notation of time. Since, the Boolean network reaches a steady state from any initial state; this approach is mainly applicable in systems where steady state is reached.

1.2.1 Stochastic Modeling

Stochastic Modeling represents a very comprehensive modeling approach in which each variable represents the number of molecules. A stochastic model is a tool for estimating probability distributions of the system over time by repeating the simulations many times. One simulation gives one potential behavior of the studied system. Distributions of potential outcomes are derived from a large number of simulations (stochastic projections) which reflect the random variation in the input. If the set of possible states is continuous then instead of probabilities stochastic process can be described by probability densities.

One of the most commonly used algorithm for simulating stochastic processes in continues time and discrete state space is the Gillespie algorithm (Gillespie, 1976). Each run makes one possible realization; repeating the simulation many times allows us to estimate the statistical properties of the process (mean behavior, time correlations, probabilities for certain kinds of behavior).

Stochastic modes describe biological processes more accurately then the Ordinary Differential Equation approach, but the main drawback is that computation time is very intensive. Due to this reason they are often replaced by deterministic calculations.

1.2 ODE models

Since in building the models for biochemical systems, often for a given input, the output has to be determine, the equations we use are deterministic (i.e there is a mapping function *f*, such that *y=f(x)*, *y* being the output, and *x* is the input values).

One of the mostly used model techniques in modeling biological systems is the Differential Equation approach. If the changes in the system are only time dependent then we consider the differential equation of type $\frac{dx_i}{dt} = f_i(x_1, ..., x_n, p_1, ..., p_l, t)$ and refer to it as Ordinary Differential Equation (ODE). The main characteristic of ODEs is that we can obtain deterministic time series for the variables under investigation. Linear ODE can be solved analytically, while non-linear ODEs are much harder, and in some cases it is impossible to find the solution analytically. In this case the approximate solution is derived using numerical algorithms for solving differential equations. One of the most elementary methods for solving ODEs numerically is Euler's forward and backwards methods (Appendix B.1).
Since in life the most interesting things are quite complicated, and we are trying to model living systems – most of the biochemical pathways are modeled using non-liner ODEs.

Here, we start by introducing the classical biochemical reaction, well – known Michaelis-Menten equation, which describes enzyme kinetics.

$$E + S \underset{k_{-1}}{\overset{k_1}{\rightleftharpoons}} ES \xrightarrow{k_2} E + P \tag{1.1}$$

Where:

E is the enzyme
S is the substrate, [S] is substrate concentration
ES is the enzyme-substrate compex
P is the product
k_1 is association of substrate and enzyme
k_{-1} is dissociation of unaltered substrate from the enzyme
k_2 is dissociation of product from the enzyme

From the scheme (1.1) we can derive system consisting of 4 ordinary differential equations:

$$\begin{aligned}
\frac{d[E]}{dt} &= k_{-1}[ES] + k_2[ES] - k_1[E][S] \\
\frac{d[S]}{dt} &= k_{-1}[ES] - k_1[E][S] \\
\frac{d[ES]}{dt} &= k_1[ES] + k_{-1}[ES] - k_2[E][S] \\
\frac{d[P]}{dt} &= k_2[ES]
\end{aligned} \tag{1.2}$$

With the following assumptions:

$[S] \gg [E]$

$\frac{[ES]}{dt} = 0$

The rate of production of product *P* is:

$$V = \frac{V_{max}[S]}{[S] + K_m} \tag{1.3}$$

The equation (1.3) is Michaelis-Menten kintics, where:

V_{max} is maximal velocity of the enzyme and $V_{max} = k_2(E + ES)$

K_m is Michaelis constant and $K_m = \frac{k_{-1} + k_2}{k_1}$

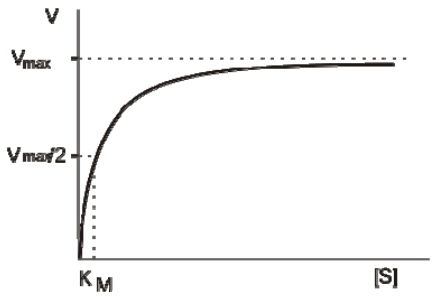

Figure 1.1| Michaelis – Menten kinetics

Obtaining the values of V_{max} and K_m, can be complicated (series of measurements of initial rates for different initial concentrations), since the rate is non-linear, the non-linear regression method should be used.

This process can be simplified by transforming Michaelis – Menten equation to obtain a linear relation between the variables. A commonly used method is Lineweaver-Burk (L-B) regression method (1.4); where V_{max} and K_m values can be obtained directly form the slope of the L-B plot.

$$\frac{1}{\boldsymbol{v}} = \frac{1}{\boldsymbol{V_{max}}} + \frac{\boldsymbol{K_m}}{\boldsymbol{V_{max}[S]}} \tag{1.4}$$

A plot, $\frac{1}{\boldsymbol{v}}$ vs. $\frac{1}{\boldsymbol{[S]}}$ yields a slope $\frac{\boldsymbol{K_m}}{\boldsymbol{V_{max}}}$ and an intercept $\frac{1}{\boldsymbol{V_{max}}}$.

It is important to note that the L-B method is very sensitive to data error and it strongly biased towards fitting the data in the low concentration range. Other methods in use are Eadie-Hofstee, Scatchard (modification of Eadie-Hofstee method) and Hanes-Woolf.

Approximation achieved with ODE models, considering very fast computational time, makes this approach widely accepted.

1.3 Parameter Estimation in ODE models

While building a model, we make many assumptions, since it is often impossible to acquire real values for all parameters. In some cases, parameters are not measurable directly, or there is inconsistency between different labs and strains that are used. In those cases, we have to estimate 'unknown' parameters by fitting the model to experimental data.

While estimating the parameters we are trying to minimize the error function over the parameters under investigation. Using the goodness of fit measure we are looking at the discrepancy between the observed values and the expected values in the model.

Most common methods for estimating parameters for the given model are the Least Square or the Regression Analysis method described by Gauss in the end of 18^{th} century and the Maximum Likelihood Estimation developed by Fisher in the beginning of 20^{th} century.

Note that the Least Square Method is the basic method for parameter estimation. There are a number of other algorithms that can be also used.

1.3.1 Least Square Method

Usually the experimental data we use when creating the model are accompanied by noise. Even though all control parameters (independent variables) remain constant, the resultant outcomes (dependent variables) vary. Therefore, a process of quantitatively estimating the trend of the outcomes, also known as regression or curve fitting, becomes necessary.

The regression process fits equations of approximating curves to the experimental data. Nevertheless, for a given set of data, the fitting curves of a given type are generally not unique. Thus, a curve with a minimal deviation from all data points is desired. This best-fitting curve can be obtained by the method of least squares.

Consider the data set consisting of n pairs (x_1,y_1), (x_2,y_2),…, (x_n,y_n), where x_i is independent and y_i is the dependent variable. Let $f(x)$ be the fitting curve and $d_i = y_i - f(x_i)$ the deviation from each data point.

Then the curve that would best fit the data would be:

$$\sum_{i=1}^{n} d_1^2 = \sum_{i=1}^{n} [y_i - f(x_i)]^2 = \text{minumum} \tag{1.5}$$

Observe that function *f(x)* can have many different forms:

a) $f(x) = ax+b$ will give The Least Squares Line method with the necessary condition of having at least 2 data pairs ($n \geq 2$).

b) $f(x)=a+bx+cx^2$ will give The Least Squares Parabola method with the necessary condition of having at least 3 data pairs ($n \geq 3$).

c) $f(x)=a_0+a_1x+a_2x^2+....a_mx^m$ will give The Least Squares m^{th} Degree Polynomial with the necessary condition of having at least $m+1$ data pairs ($n \geq m+1$).

If we consider the simplest regression – The Least Square Line method, the best fitting curve will be:

$$\sum_{i=1}^{n} d_1^2 = \sum_{i=1}^{n} [y_i - (a + bx_i)]^2 \tag{1.6}$$

In order to calculate values for *a* and *b*, the first derivative of equation (1.6) needs to be equal to zero:

$$\left(\sum_{i=1}^{n} [y_i - (a + bx_i)]^2 \right)' = 0 \tag{1.7}$$

Follows:

$$a = \frac{\left(\sum_{i=1}^{n} y_i\right)\left(\sum_{i=1}^{n} x_i^2\right) - \left(\sum_{i=1}^{n} x_i\right)\left(\sum_{i=1}^{n} y_i x_i\right)}{n\left(\sum_{i=1}^{n} x_i^2\right) - \left(\sum_{i=1}^{n} x_i\right)^2}$$

$$b = \frac{n\left(\sum_{i=1}^{n} y_i x_i\right) - \left(\sum_{i=1}^{n} x_i\right)\left(\sum_{i=1}^{n} y_i\right)}{n\left(\sum_{i=1}^{n} x_i^2\right) - \left(\sum_{i=1}^{n} x_i\right)^2} \qquad (1.8)$$

In the similar way we can calculate values for parameters *a, b* and *c* in the case of *Parabolic* method or set of parameters, $a_0,\ldots,a_m$ in the m^{th} *Degree Polynomial* method.
It is important to note that if the distribution of experimental error is normal then the least square estimator is maximum likelihood estimator.

1.3.2 Evolutionary Strategy

Parameter Estimation in biochemical modeling usually involves more complex algorithms then the Least Square Method. Mani problem is the impossibility to unambiguously determine all parameters from the considered data set. The question often asked is: Can parameters of an ODE model in theory be identified for different sets of input/output parameters? Since, minimization in principle is hard optimization problem for models of realistic size and complexity (several local minima), it can be solved by setting the boundaries for parameters. Avoiding local minima problem of the error function can be solved using global methods. *More et al.* (2003) tested 7 different global optimization methods. The challenge was to find the optimal method for problems involving large search space with ODEs that are highly non-linear in the variables and parameters. Out of 7 tested methods six were stochastic and only one deterministic. The

best result in obtaining the true parameters was accomplished with the SRES method. One of the best and most widely used is an Evolutionary Strategies based algorithm, namely Evolutionary Strategy using Stochastic Ranking (SRES, *Runnarsson et al. 2000*). Stochastic Ranking is based on a bubble-sort algorithm and is supported by the idea of dominance. During the evolutionary search the balance between the objective and penalty function is automatically obtained. Problem with this method that it has a worst-case complexity $O(n^2)$.

1.4 Sensitivity Analysis

As shown earlier, designing a mathematical model for biological systems is a circular process, where the main focus is on the parameters and the variables that are characterizing the chosen process.
The simplest definition of sensitivity analysis would be that we are observing the effect on the system after changing the parameters.
Together with parameter estimation, systems analysis is one of the most important and at the same time the most difficult and laborious steps in modeling procedure.

Performing the sensitivity analysis we can get more information about our model. Some of the questions usually asked are: which parameters have the highest influence on system behavior or on the other hand which ones do not have any effect on the system, so they don't have to be considered further and can be fixed to some arbitrary value.

The main goal of sensitivity analysis is to better understand the dynamic behavior of the system.

Due to the difficulties in obtaining the quantitative values of certain parameters or if the modeler is not certain when choosing some parameter values, it is necessary to use estimates. Sensitivity analysis will ‘show’ the level of accuracy of parameters one should use to make a model that is useful and valid. Experimenting with a wide range of values will lead us into behavior of a system in extreme situations. Discovering that the system behavior greatly changes for a change in a parameter value, we can identify a parameter whose specific value can significantly influence the behavior mode of the system.

As we already noted, sensitivity usually refers to single parameter changes: how does input signal *x* change output signal *y*. This can result in 3 levels of sensitivity:

1. High sensitivity
   x has a strong effect on *y* (usually implies that is hard to estimate values for *x*)
2. Low sensitivity
   x has a no effect on *y* (usually implies that is easy to estimate values for *x*)
3. Negative sensitivity
   x inhibits *y*

In the second scenario we generally refer to as a robust system (*y* is robust against the changes of *x*).
In contrast to single parameter change, it is possible to change several parameters at once. Then we have multiple parameter change and the combined effect can simply be measured by summing up the single effect. Note that this holds only in case that parameter changes are sufficiently small.

1.4.1 Robustness vs. Sensitivity

In some case it is expected that the input parameter doesn't affect the output greatly, which can confirm the behavior of the system and on other hand the system is expected to be sensitive to certain parameters. It is wrong to assume that only sensitive parameters are 'good' ones and the ones that can give you the most information about the system. In many cases, as practice has proved, the robustness is also necessary in order to validate the model.

A large number of sensitivity analysis methodologies are available in the literature. Like any method in use, different sensitivity analysis methodologies have their advantages and disadvantages. Choosing the right method for performing a sensitivity analysis experiment on a model is therefore a very delicate step that depends on a number of factors: the properties of the model, the number of input factors involved in the analysis, the computational time needed to evaluate the model or the objective of the analysis.

1.4.2 Overview of common sensitivity measures

Consider the mathematical model: $F(u,k)=0$, where k is a set of m parameters and u is a vector of n output values (McRae et al. ,1982).

Then, the following sensitivity measures can be used:

1. Response from arbitrary parameter variation

$$u = u(\bar{k} + \delta k) - u(k)$$

2. Normalized Response

$$D_i = \frac{\delta u_i}{u_i(k)}$$

1. Variance

$$\delta_i^2(k) = \left\langle u_i(k)^2 \right\rangle - \left\langle u_i(k) \right\rangle^2$$

2. Extrema

$$max[u_i(k)],\ max[u_i(k)]$$

These measures are often use when the model is run for a set of sample points (different combinations of parameters).

1.5 Standardization of biochemical models

The rapid development in the field of systems biology led to enormous expansion of computational tools that can be used for system analysis. Most of the tools are freely available for the scientific community and their use will greatly depend on the user's preferences and expertise (*Klipp et al., 2007*).

The vast amount of mathematical models resulted in a need of creating standards for their systematic organization. One such standard is MIRIAM - Minimum Information Requested in the Annotation of biochemical Models. It is composed of three parts: *reference correspondence*, *attribution annotation*, and *external resource annotation*. Each of these 3 parts deals with specific requirements which a standardized model has to fulfill. The model has to be encoded in a standardized machine – readable format, where all the components have to be defined and annotated appropriately using Uniform Resource Identification (URI).

Standardization of machine-readable format is achieved through Systems Biology Markup Language (SBML). It is an XML based language and the main purpose is encoding and exchanging quantitative biochemical models in Systems Biology. The original specification (Level 1) aimed mainly at continuous deterministic models. Whereas, the current specification (Level 2) is perfectly capable of encoding discrete stochastic models in an unambiguous way.

Models of arbitrary complexity can be represented and each type of components is described using specific data types. More information regarding structure, development and additional tools is available on the developer's web site www.sbml.org.

Age is an issue of mind over matter. If you don't mind, it doesn't matter.

Mark Twain

2. Biology behind equations

2.1 Ageing: definitions and history

Aging is the process, which intrigues people since the ancient time. Finding the aging formula and a possibility of controlling it represents the incredible challenge and motivation. One of the first fictions written - *Epic of Gilgamesh* - has a main focus on immortality. History is full of individuals whose life was driven by the force of finding the *fountain of youth* – a legendary spring that restores the youth. And where we are today? Are we just modern Gilgamesh, with improved tools, techniques and hopefully more knowledge, but with the same goal? Is it true that we want to live indefinitely? Laws of physics are pretty simple and sometimes harsh: "over time differences in temperature, pressure, and density tend to even out in a physical system that is isolated from the outside world". This is the Second Law of Thermodynamics and in principal explains irreversibility in nature. So, immortality, defined as 'possibility of repair and incapability of dying' is not possible. The other term in use, *indefinite lifespan*, might be more appropriate, since it implies freedom from death by age.

What is then our goal? To make old people healthier. As simple as that. To have a generation that will enjoy in their elderly life, without being burden for society. Already today, there is evidence to suggest that not only are we living longer, we are staying healthier until an older age - something health experts refer to as 'compression of morbidity', meaning that most of us will only suffer severe age-related illnesses in the last years of life.

Defining ageing is complicated as the ageing process itself is. There is no *the definition*, but rather a series of descriptive observations which together can give us some glimpse how we see the ageing phenomena. One of the descriptions commonly used is that 'ageing is simply the age or time dependent changes that occur to biological entities' (*Medawar, 1952*). But, this doesn't give us an answer how and why changes arise.

2.2 Yeast as a model organism

To come closer of solving the mystery of human ageing, we have to start from simpler organisms. Yeast in general has been accepted as very powerful model to study various biological processes. Advantages are numerous: it is relatively easy to culture them, do genetic manipulations, experimental tools to analyze their biochemical and physiological functions are established. Of the great importance is the fact that it has its full genome annotated, that generation time is fast, and also very important aspect that is relatively cheap to use.

In the course of this work, two yeast species were studied *Saccharomyces cerevisiae* and *Schizosaccharomyces pombe*.

2.3 Cell division

2.3.1 Asymmetricaly dividng systems - *Saccharomyces cerevisie*

Saccharomyces cerevisie (baker's yeast or budding yeast) is one of the simplest eukaryotic organisms. In the spring of 1996, the complete genome sequence of the *S. cerevisiae* was obtained, making yeast the first eukaryotic organism to be completely sequenced.

It is a small, single-cell fungus. Like other fungi, it has rigid cell wall and mitochondria but not chloroplast. It reproduces almost as fast as bacteria. Most fundamental cellular processes are conserved from *S. cerevisiae* to humans and have first been discovered in yeast. There are many basic biological properties that are shared. About 20 percent of human disease genes have counterparts in yeast. This suggests that such diseases result from the disruption of very basic cellular processes, such as DNA repair, cell division or

the control of gene expression. It also means that we can use yeast to look at functional relationships involving these genes, and to test new drugs.

S.cerevisiae divides in a way that is not very common in nature. Buds (future 'daughter' cell) may arise at any point on the existing cell surface (referred to as 'mother). Buds are formed when the mother cell has attained a critical size. After cell division a characteristic bud scar is left on the surface of the mother cell (Figure2.1).

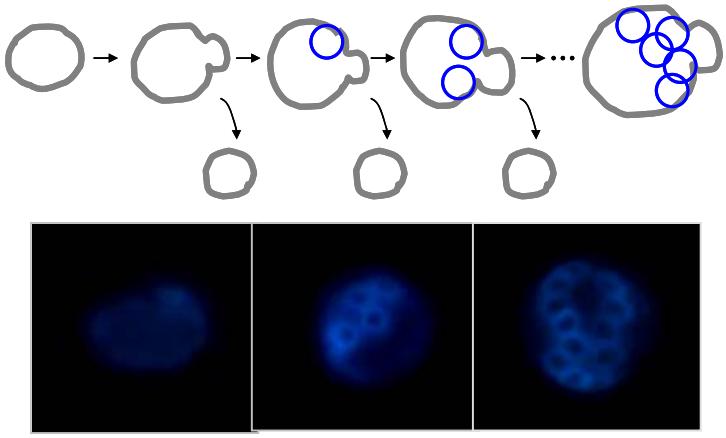

Figure 2.1| Accumulation of bud scars. Upper panel is schematic representation of bud scars appearance on mother's cell surface during successive division. Lower panel is calcoflour staining of bud scars (graphical representation courtesy of Nika Erjavec).

Since the new born daughter has a smaller size then its mother, it will require longer generation time to attain a critical size before it in turn becomes mother itself (Figure2.2). However, this unconventional way of division and clear asymmetry between mothers and daughters, makes it an excellent model for studying ageing. But this is not the only prerequisite for studying ageing. Bakers yeast has been established as model for cellular ageing in 1959 when Mortimer and Johnston discovered that individual yeast cells are mortal.

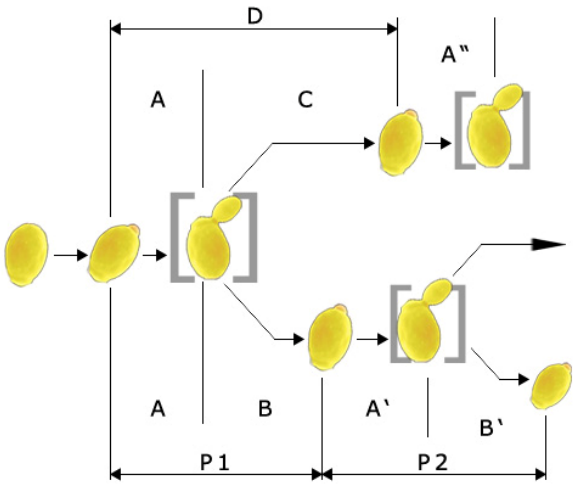

Figure2.2| Generation time in S.cerevisiae; P1 - first parent generation; P2 - second parent generation; D - daughter generation time; A - division of the parent from the bud in 1st parent generation; A'- in 2nd division, A''- division of daughter from its 1st bud. Generation time is the period between the appearance of the first and the second consecutive buds on a given cell. Generation time increases with age, especially after 18 to 20 generations

2.3.2 Symmetricaly dividing systems - *Schizosaccharomyces pombe*

In 2001 the *Schizosaccharomyces pombe* genome was reveled. This achievement showed that *S.pombe* is functionally and structurally more similar to humans then *S.cerevisiae*. This made *S.pombe* another alternative model organism. Since, the *S.pombe* genome has an evolutionary different origin then that of *S.cerevisiae*, they can be seen as complementary model systems. Processes conserved in both can have mechanisms that evolved in similar fashion and can be used for studies in other higher eukaryotes.

Schizosaccharomyces pombe divides by binary fission. A cell septum, when formed, constricts the cell into two equally sized siblings. Growth of *S. pombe* will first take place at the old end and subsequently also at the new end. The latter growth period is called New End Take Off or NETO (Figure2.3).

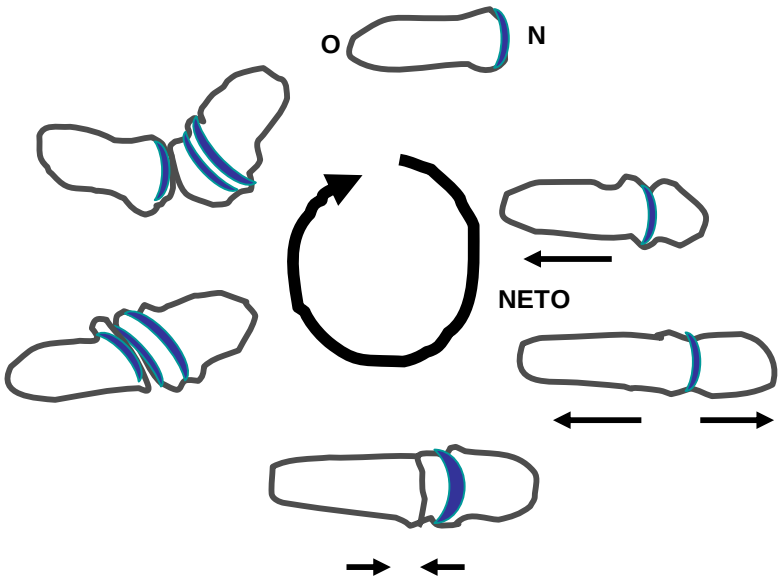

Figure2.3| Growth of Schizosaccharomyces pombe. Schematic representation of *S.pombe* progression through cell cycle. In blue accumulation of bud necks is presented. (graphical representation courtesy of Nika Erjavec).

2.4 Ageing in Yeast

As previously noted, ageing in *S.cerevisiae* has been reported 50 years ago. Yeast shows the same exponential decline in fitness and fecundity over time, as many other higher eukaryotes. The mortality curves follow the Gompertz-Makeham law (see Chapter 3 for more details) (Figure2.4).

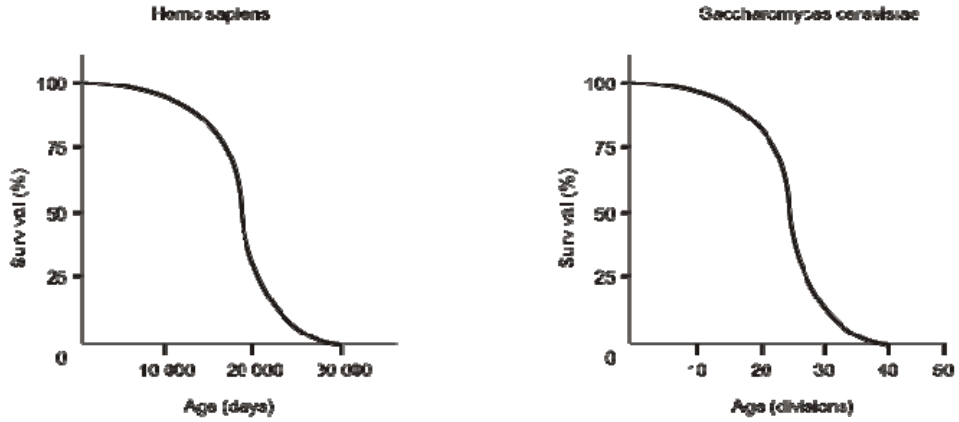

Figure2.4| Mortality curves. Survival by age, know as mortality curve, for humans and yeast.

Yeast lifespan can be measured in two ways:

Replicative lifespan is defined as the number of divisions an individual yeast cell undergoes before dying. It is expressed in generations (it is limited) and it is measured by growth on agar plates and micromanipulation. (Figure 2.5A)

Chronological lifespan (survival in stationary phase), is the time a population of yeast cells remains viable in a non-dividing state following nutrient deprivation. It is expressed as time and measured by growth in liquid. (Figure 2.5B)

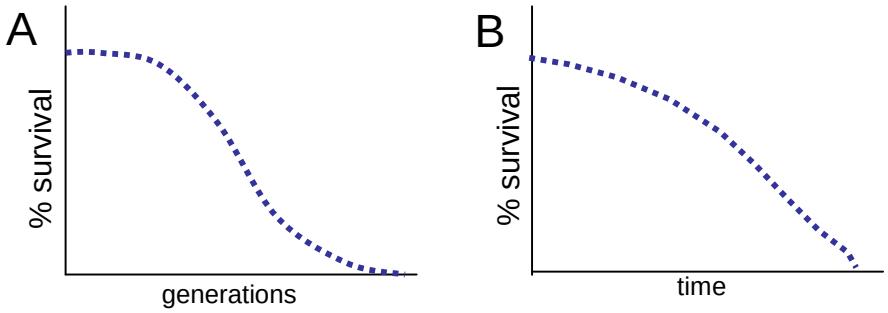

Figure2.5| Replicative and chronological life span in yeast.

There is no strong correlation between chronological and replicative lifespan. It has been shown that the chronological lifespan can be noticeably extended without altering the replicative lifespan.

When studying yeast ageing we are mainly focused on replicative lifespan.

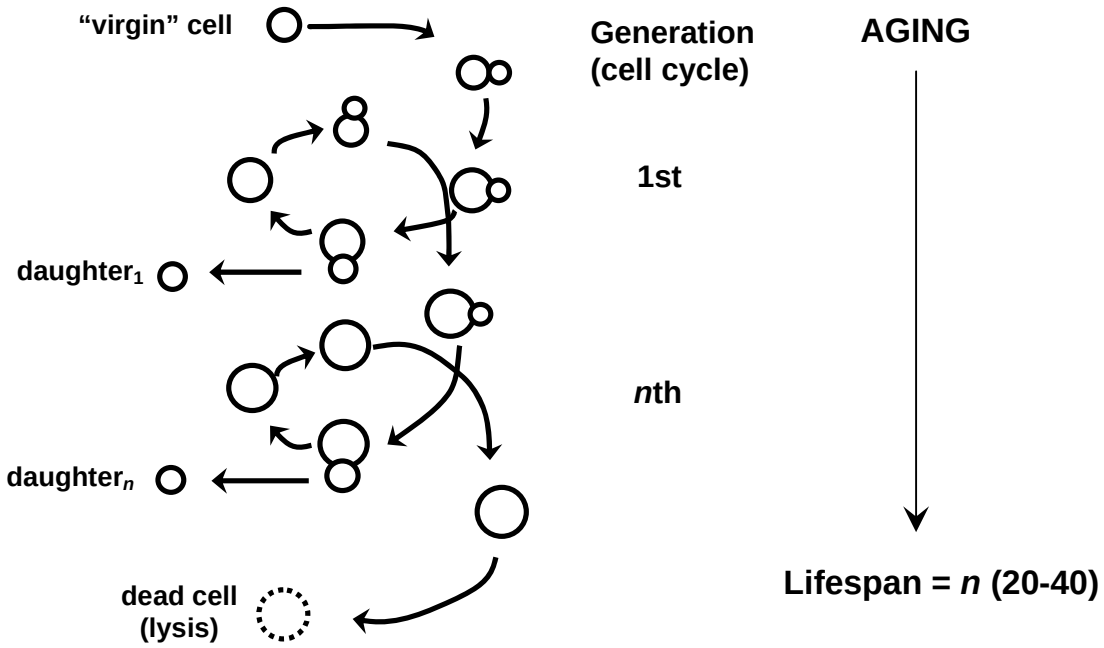

Figure 2.6| The spiral model of yeast ageing (Adapted from Jazwinski, et al *Exp Geront* **24**:423-48 (1989))

From the mortality curves we can define mean and maximum lifespan:

Mean lifespan (average lifespan) corresponds to the age at which the horizontal line for 50% survival intersects the survival curve.

Maximum lifespan corresponds to the age at which the survival curves touch the age-axis (0% survival) - and this represents the age at which the oldest known member of the species has died.

For wild-type (wt) laboratory yeast strain, the mean lifespan is approximately 25 divisions, while the maximal is around 40 (Figure2.6). Those numbers should not be taken too exact, since lifespan can vary due to the numerous reasons: different labs, different strains.

A mother cell undergoes many typical changes during her life time, such as: sterility, slowing of the cell cycle, appearance of surface wrinkles, blebs and bud scars, dramatic increase in cell size, loss of asymmetry, fragmentation of nucleus.

It has been believed that the accumulation of bud scars can limit the replicative potential in yeast. However, buds occupy only 1% of the mother's surface, and even expanding the available surface would not lead to an increased lifespan. Also, there are reports that new buds can grow from existing scars.

One of the most obvious signs of an old yeast cell is the increase in size. Several studies showed that the volume of a mother cell increases linear with age. Along with size, cell cycle increases exponentially with generation time, as well.

Due to the clear size-symmetry, *S.pombe*, was not considered as ageing model until 1999 when it was reported that fission yeast has a finite lifespan.

It was believed that this organism doesn't age, since the division is symmetrical, and the two produced siblings will be completely identical. The similar arguments were applied for bacterium *Escherichia coli.* Recent work by *M. Ackermann* (2003) and *E. Stewart* (2005) purposed that *Caulobacter crescentus* and *E.coli* display replicative senescence e.g. one sibling stops dividing after accomplishing certain number of division, while the other continuers to divide normally.

“Tomorrow you may be younger.”

2.5 Ageing theories

Since the beginning of ageing research more then 300 theories have been postulated. The key requirement for a good ageing theory would be the necessity of having high predictive and explanatory power. At the beginning of ageing research scientist were looking for the one and only theory – *the theory* – the one that would give complete understanding of the highly complex ageing process. Even there have been discussion could we called it *ageing process*? Is it a *process*? By general definition *process* is “a series of actions, changes, or functions bringing about a result” it can also be “a natural phenomenon marked by gradual changes that lead toward a particular result”. The common thing for all those definitions is that it is something that has a beginning and an end. And ageing indeed has a starting point – new cells are created over and over again, and an end point is the death of the cell itself. Death as a final result of series of changes that cell goes through.

In general, ageing theories can be summarized in two groups:

1. Programmed Theories
2. Error Theories

The main idea behind Programmed Theories is that cells are designed to age. Ageing is due to something inside an organism's control mechanisms that forces elderliness and decline.
The other, more accepted – Error Theory postulates that ageing is caused by environmental damage to the cells, which accumulates over time. It can be damage due to radiation, chemical toxins, metal ions, free-radicals, hydrolysis, disulfide-bond cross-linking, etc. Such damage can affect genes, proteins, cell membranes, enzyme function and blood vessels.

One of the first Error Theories was Orgel's Error Catastrophe (1963). The theory suggests that copying errors in DNA and the incorrect placement of amino acids in protein synthesis could aggregate over the lifetime of an organism and eventually cause a catastrophic breakdown in the form of obvious aging. This theory has been dismissed since the experimental verification always gave negative results.

Other error theories include *wear and tear theory* – cells and tissues simply wear out over time, *rates of living* – the oxygen usage is faster in some organisms, therefore they live shorter.

In this chapter will give brief overview of some of the most studied and further developed theories.

2.5.1 Free Radical theory

Following the idea of *R. Gerschman* that free radicals are toxic agents, *D. Harman* purposed in 1954 the Free Radical Theory of Ageing. In general, this theory presumes that there is an accumulation of free radicals over time. Under the name *free radicals* we often assume *reactive oxygen species* (ROS). ROS molecules are highly reactive and as such can damage all sorts of cellular components. The ability to cope with ROS decreases with age. One form of this theory – accumulation of damaged proteins is discussed in section 2.6.

2.5.2 Disposable soma theory

Based on the fact that both somatic maintenance and reproduction require energy, the disposable soma theory postulates that there is a negative correlation between reproduction and repair. This theory predicts that aging is due to the accumulation of un-repaired somatic defects and the primary genetic control of longevity operates through selection to increase or decrease the investment in the basic cellular maintenance systems in relation to the level of environment hazard. Also, a high level of accuracy is

maintained in immortal germ line cells, or alternatively, any defective germ cells are eliminated.

2.5.3 ERCs

In 1997, *Sinclair* and *Guarente* proposed that yeast ages due to gradual accumulation of extrachromosomal ribosomal DNA circles (ERCs). In *S.cerevisiae* ERCs are located on the XII chromosome. Unsilenced rDNA have an increased frequency of recombination events and homologous recombination in this region can lead to the formation of extrachromosomal rDNA circles (ERCs). Since ERCs contain an origin of replication, they can self-replicate (Figure 2.7). Interestingly, ERCs are asymmetrically inherited by the mother cell at the time of cytokinesis. Furthermore, overexpression of ERCs shortens lifespan (*Sinclair and Guarente, 1997*). Therefore, ERCs have been proposed to be a senescence factor.

Deletion of ribosomal DNA (rDNA) repeats results in the formation of ERCs. Since ERCs are able to replicate independently during S-phase, they can accumulate much faster then chromosomal DNA. During the budding process ERCs are retained in the mother cell, leaving the daughters ERC-free, which in turn give an immortal yeast population. When a mother cell gets close to its replicative life, the mechanism for ERC segregation starts malfunctioning which results in daughters that inherit small amounts of ERCs. Because, the level of ERCs is still too low, this prematurely old daughters are capable of producing healthy daughters.

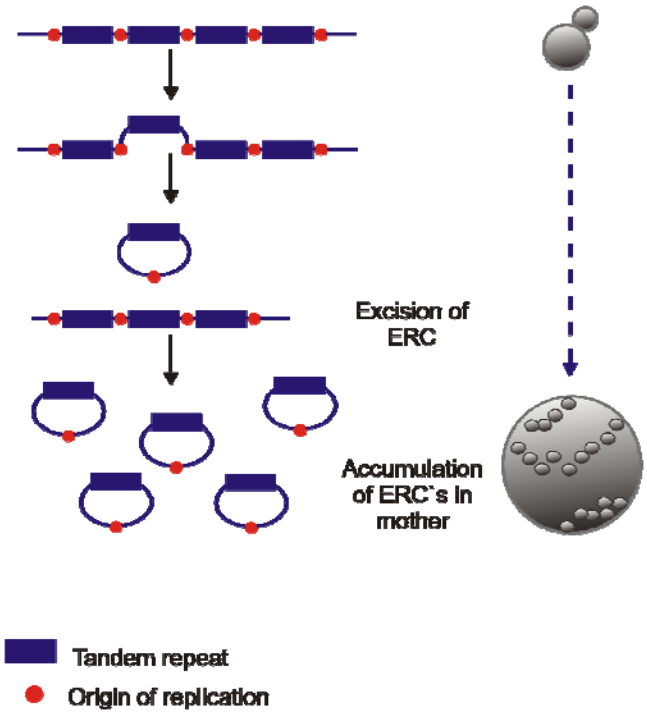

Figure2.7| Formation of extrachromosomal ribosomal DNA circles (ERCs). In budding yeast ERCs are accumulated over mother cell life span and are segregated asymmetrically between progeny and progenitor.

The reason why this theory is not widely accepted is the fact that ERCs accumulation is only observed in *S.cerevisiae* and it is believed that it can not explain ageing in higher eukaryotes.

2.6 Accumulation of damaged proteins

The Free Radical Theory indicates the key role of ROS in the ageing process. ROS damages cellular components and can cause oxidative damage to cellular macromolecules (proteins, carbohydrates, lipids and nucleic acids) which in turn become cytotoxic. According to Free Radical Theory, ageing is caused by the gradual accumulation of un-repaired molecular damage, leading to an increasing fraction of damaged cells and, eventually, to functional impairment of tissues and organs.

Native proteins can become reversibly and/or irreversible oxidatively damaged. The reversible ones are repaired by specific enzymes. The repair mechanism is present in cytosolic and mitochondrial compartments. The rest of the proteins are irreversibly damaged and there is no evidence of their repair mechanism. They are eliminated either via degradation pathways or become aggregates. The degradation pathways are part of the cytosol and mitochondria and are regulated by 20S proteasome, lysosome and Lon protease respectively (Figure2.8).

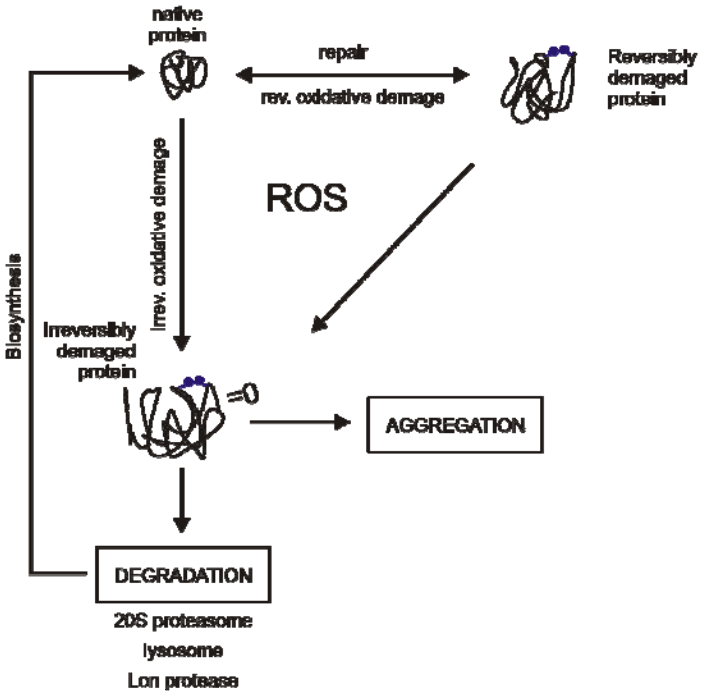

Figure2.8| Different modes of protein degradation.

An age - related increase in the level of oxidatively modified proteins disrupts the balance between the rate of protein oxidation and the rate of elimination of oxidized proteins. As long as the balance is kept the cell is viable.

Protein carbonylation negatively affects cellular performance in two ways; (i) the modification causes structural aberrancies and abrogates the targeted proteins' catalytic

functions and (ii) triggers formation of high molecular, potentially cytotoxic, aggregates that, among other things, may impede protease activity.

Inability of the cell to eliminate oxidatively damaged proteins causes the buildup of damaged proteins, which becomes a burden for the cells and lead to cell death.
Increase in oxidatively damaged proteins with age has been shown to occur in a variety of species, including mammals, birds, bats, nematodes, flies, budding yeast, and non-growing bacteria. (Figure2.9)

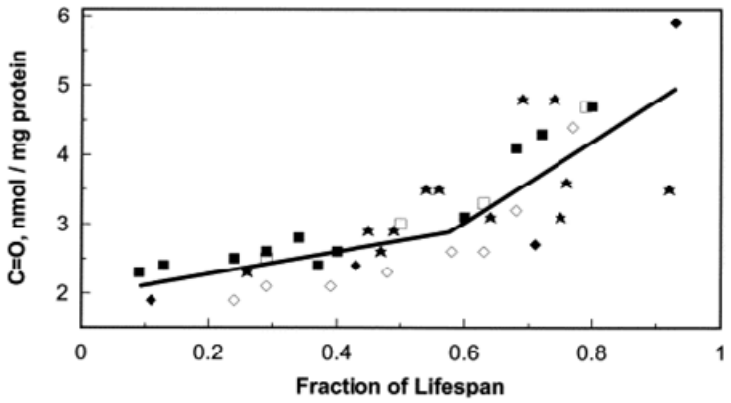

Figure2.9| Increase in oxidatively damaged proteins with age. A dramatic increase in oxidized protein during the last third of the lifespan can be observed. The data points were taken from published reports: ▪ human dermal fibroblasts in tissue culture; ★ human lens; □ *C. elegans*; ♦ rat liver; ◦ fly. (Taken from *R. Levin, 2002* with the permission from publisher).

The load of oxidatively damaged proteins will inevitably lead to a reduced replicative life span.

2.7 Damage retention

Accumulation of oxidized proteins has been shown to occur during mother cell-specific ageing, starting during the first G1 phase of newborn cells.

It has been shown that oxidatively damaged proteins are inherited asymmetrically during yeast cytokinesis such that most damage is retained in the mother cell (*H. Aguilaniu*, 2003) (Figure2.10). In other words, proteins that are oxidatively damaged are retained within the mother cell, leaving its daughter virtually damage free. The process was shown to be dependent on the age determinator *SIR2* and on actin polymerization. Deletion of *SIR2* shortens the replicative lifespan while its overexpression prolongs lifespan.

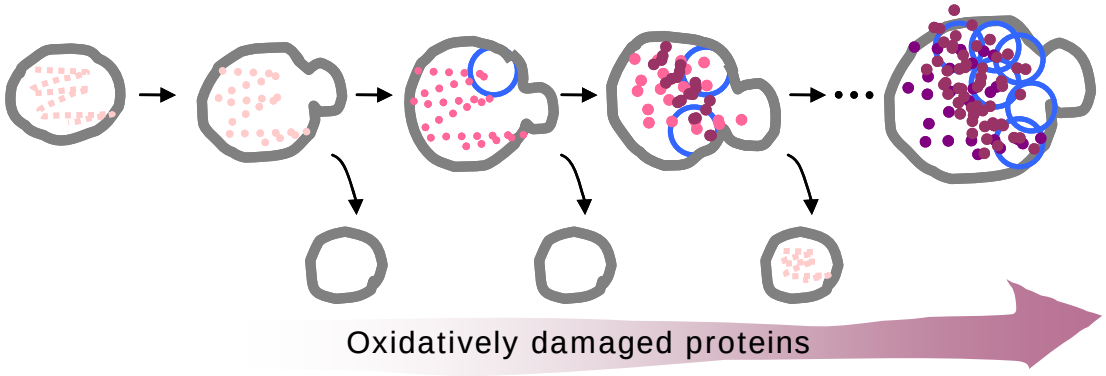

Figure2.10| Schematic representation of asymmetrical accumulation of damage proteins during replicative age in S.cerevisiae. Light pink dots represent low level of damage, while darker dots show high level of damaged proteins. (graphical representation courtesy of Nika Erjavec)

The fact that yeast has a limited replicative lifespan implies that each daughter cell produced must have a full replicative potential. Thus, there is a critical asymmetry at the time of cell division that ensures the proper segregation of a "senescence factor" (*Egilmez et al.*, 1990). The nature of this factor is still under intense scientific scrutiny.

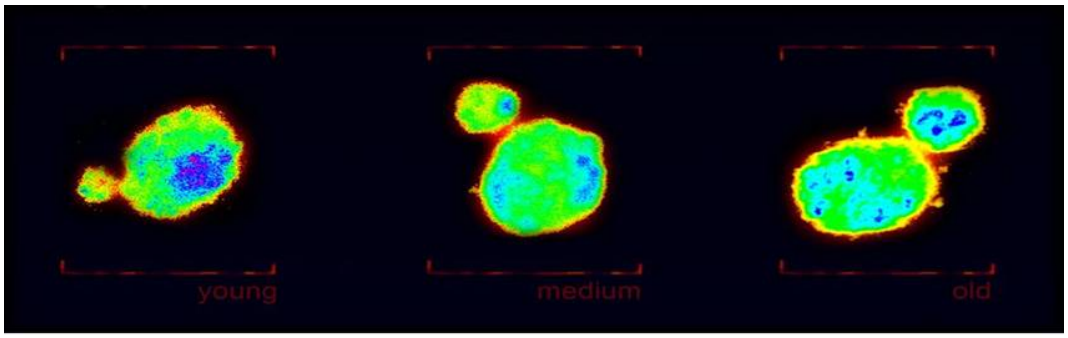

Figure2.11| Asymmetric distribution of oxidized proteins during cytokinesis in S.cerevisiae. Representative young, 4-5 and 10.12 generations old dividing mother cell. Oxidized proteins are detected in situ and here are increasing from red to blue.

In *S.cerevisiae* age-dependent oxidation targets most proteins and most oxidized proteins are accumulated to the same extent in the mother cell. Segregation of oxidized proteins is a result of active retention in the mother cell.

Overall double increase in carbonylation in old mothers and in the daughters of old mothers, compared with unsorted culture, implies that asymmetric distribution of oxidatively damaged proteins take place between mother and bud in aging yeast cells. (Figure 2.11 and Figure 2.12).

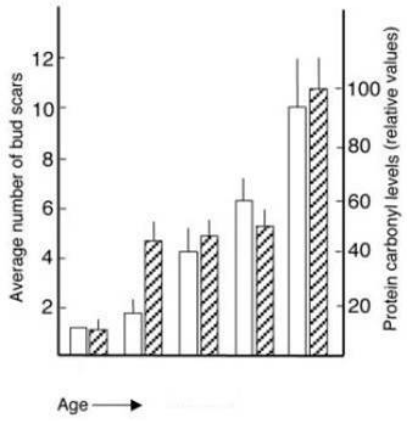

Figure2.12| Levels of oxidative protein damage as a function of replicative age. Average number of birth/bud scars (open bars); Protein carbonyl levels (filled bars). Taken from *H. Aguilaniu* (2003) with the permission from publisher.

2.8 Rejuvenation

The verb *rejuvenation* (*re* + Latin *juvenis* – young) means to become/make young or youthful again. Rejuvenation, even though opposite from ageing, complements the ageing process and is an inevitable aspect of aspiration to have an immortal population.

The altruistic concept of having a system that will for the benefit of the population entrust the off-spring that is intact of any sort of damage is one of the most striking biological phenomena.

The whole concept of ageing research can then be formulized in one yet obvious, but very complex question: "How something old can generate something young?"(*Thomas Nyström*)

In *S.cerevisiae*, as previously stated, a mother cell produces an off-spring that is born damage-free with full replicative potential.

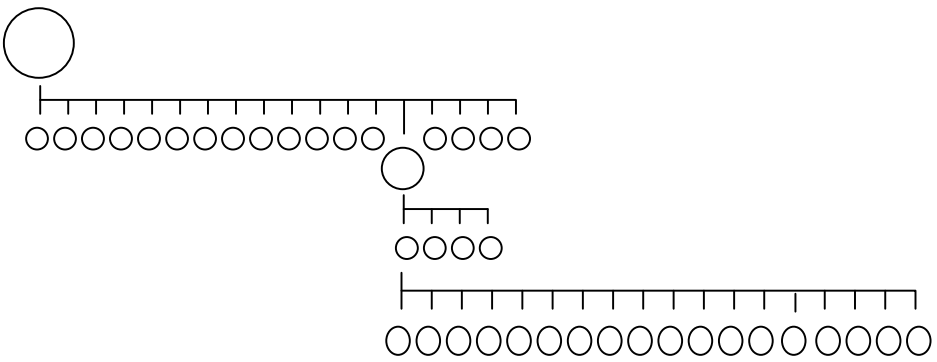

Figure2.13| Rejuvenation. The old mother cell produces a prematurely old daughter, whose replicative potential is equal to the remaining mother's life span. Remarkably, daughters born from these old daughters, display normal replicative life span.

As a mother cell becomes older, the newly produced daughters are born prematurely old – indicating that asymmetry in protein damage, together with loss of size asymmetry has broke down. This suggests that daughters of old mothers have inherited a *senescence factor*. However, the striking thing is that the daughter of prematurely old daughters will have full replicative potential and no damaged proteins (Figure2.13)

3. Modeling Ageing in Yeast

3.1 ERC model

A mathematical model of Extrachromosomal Ribosomal DNA Circles (ERCs) accumulation in yeast developed by *Colin Gillespie*, relays on observations from *D. Sinclair and L. Guarente* that the number of ERCs is unevenly distributed between mother and daughter cell during replicative age.

The biological description of this process is given in Chapter 2.

Here we give mathematical interpretation based on the Gillespie model. The ERC model is stochastic model composed of 3 main parts.

1. ERC generation:

   The cell can acquire the ERC in 2 different ways:

   a) through excision from the chromosome
   b) through inheritance from its mother

The first step is known to appear randomly with low frequency. It holds that

$$P_{for} = \min(\alpha_i x^i, 1), \text{ for } i = 0, 1, 2 \qquad (3.1)$$

P_{for} is the probability of generating new ERC in a ERC-free mother cell

x is the number of completed generations

α_i is a constant

Introducing generation constrains, we can obtain 3 possible cases (Figure3.1):

$i = 0$ → means that the probability of generating ERCs is age-independent.

$i = 1$ → means that the probability of generating ERCs has a linear increase with age

$i = 2$ → means that the probability of generating ERCs has a quadratic increase with age

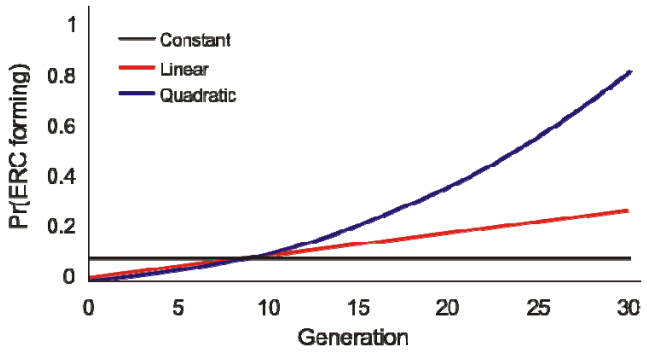

Figure3.1| Formation of ERCs

2. ERC replication; occurs during successive generations of mother cells

When an ERC is introduced into a virgin cell, the cell senescence starts after 15 generations. It is believed that after 15 generations, the cell contains 500 to 1000 ERCs.

The assumption is that replication of ERCs has a constant probability P_{rep} per ERC/cell. Such a high number of ERCs would lead to death by overcrowding.

3. ERC distribution; occurs between mother and daughter cell at the division

The asymmetrical distribution of ERC between mother and daughter is the key fact in yeast ageing. The mother cell will keep ERCs in almost 80% of all divisions; however it is known that towards the end of her replicative life, ERCs will 'leak' to her daughters, making them prematurely old.
The model assumes 2 types of ERC segregation:

a) The probability of retaining ERCs is constant and independent of other ERCs.
   If N denotes the number of ERCs in the mother cell and R denotes number of ERCs retained in the mother cell after division, then R will have a binomial distribution: $Bin\ (N_{max}, \theta_1)$

b) The number of ERCs can be retained with 2 different probabilities.
The first N_{max} ERCs are retained with probability θ_2, and above N_{max} with probability 0.5 (equal distribution of ERCs between mother and daughter), then

$$R = \begin{cases} R_1 & \text{if } N \leq N_{max}, \\ R_1 + R_2 & \text{otherwise,} \end{cases} \tag{3.2}$$

And, R_1 and R_2 have two independent binomial distributions:
$Bin(N_{max}, \theta_2)$, $Bin(N - N_{max}, 0.5)$, respectivly.

The results suggest that having a quadratic increase in probability would fit the best to experimental studies. (Figure 3.2)

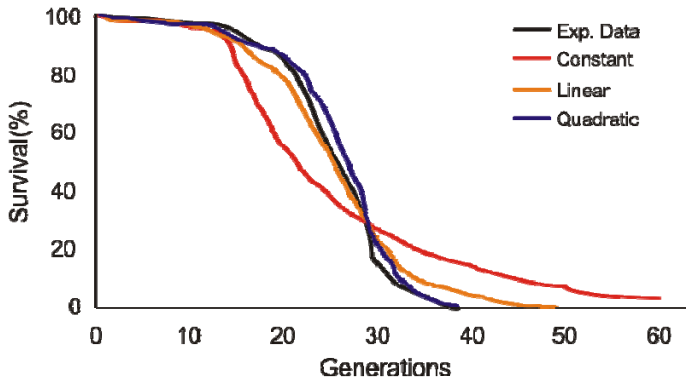

Figure 3.2| Agreement with experimental data.

Also, the segregation of ERCs breaks down in older mother cells and the formation of ERCs cannot be constant (red curve; gives long lived cells (~120 generations), but rather depends on the age of the yeast cell. This suggests that there must be another mechanism(s), in addition to ERC accumulation which underlies yeast ageing.

This theory can explain the fact that an old mother will give rise to old daughters, and that a daughter of an old daughter will have full replicative potential (e.g. born ERC-free).

3.2 Disposable Soma model for Ageing

The main aspect of the Disposable Soma theory is that there is a balance between somatic maintenance, reproduction and growth *(Kirkwood*, 1977). In Chapter 2 there is a insight to the biological background of the mathematical model developed by *Kirkwood* and *Drenos* (2004).

The Disposable Soma model is based on Euler- Lotka (1) and Gompertz-Makeham (3) equations.

3.2.1 Euler – Lotka equation

Linking the proportional growth rate of a population to the characteristic functions that define life history is an old problem, originally solved by Euler (1760), rediscovered in the context of modern population genetics by Lotka (1907), and first applied by Fisher (1930). Surprisingly, the problem has no algebraic solution, and *r* must be defined implicitly by an integral equation. The parameter *r* was dubbed by Fisher the Malthusian parameter, and the equation from which it is computed is referred to as the Euler-Lotka equation:

$$\int e^{-rx} l(x,s) m(x,s) dx = 1 \qquad (3.3)$$

Where:

r is intrinsic rate of natural selection
$l(x,s)$ is survivorship function (a proportion of population remaining alive at age x), depends on maintenance s
$m(x,s)$ is fertility function (the mean number of offsprings produced per time unit time at age x), depends on maintenance s

If we assume that *r* is known, then we can compare the relative contributions to growth of offspring produced at different times: their value declines exponentially with time at the prescribed rate *r*. The *r* is then, the rate which reduces the total reproductive value of all offspring to unity.

With computational techniques that have become commonplace, the numerical determination of *r* is fast and straightforward. The algorithm is seeded with a first guess for *r*, which is used to evaluate the integral numerically. The difference between the computed result and unity is fed into a Newton-Raphson or equivalent algorithm for generating a next-closer value of *r*, and the procedure is iterated until the desired accuracy attains.

Hamilton (1966) showed that the selection pressures acting on life history are best measured by the sensitivity of *r* to changes in fecundity or instant survival rate.

Alleles that influence life history such that *r* is increased spread at a faster rate than other alleles and invade the population. Alleles acting late in life experience affect ***r*** less strongly and thus experience a weaker selective pressure than alleles acting early in life.

This has three evolutionary consequences:

(1) Alleles that increase early survival or fertility at the cost of late survival or fertility tend to be favored.

(2) Deleterious alleles that decrease early survival or fertility will be more strongly selected against than alleles that decrease late survival or fertility.

(3) Beneficial alleles that increase early survival or fertility will be more strongly favored than alleles that increase late survival or fertility.

Consequently, it is expected that the survival or fertility rate will decrease with age (at least once sexual maturity is reached).

3.2.2 Gompertz – Makeham law of mortality

In 1825 *Benjamin Gompertz* proposed that death rate exponentially increases with age:

$$m(x) = A_0 e^{Gx} \tag{3.4}$$

Where:

$m(x)$ is mortality rate as a function of time or age
A_0 is extrapolated constant to birth or maturity (basal vulnerability)
G is exponential Gompertz mortality rate coefficient (acturial ageing rate)

Often, A_0 is replaced with A – the initial mortality rate (IMR), and G with the mortality rate doubling time (MRDT), equal to ln2/G. In humans MRDT is 8 years, meaning that after our sexual peak, chances of dying double every 8 years.
This version of Gompertz law is used in protected environments, such as laboratory conditions, where the probability of external causes of death is low. If, we are looking for the mortality rate in natural environment then, a new parameter need to be included in the equation – the Makeham parameter M_0, which then represents, the age – independent component of the Gompertz – Makeham equation (3), in the contrast to the Gompertz function which is an age-depended component.

$$m(x) = A_0 e^{Gx} + M_0 \tag{3.5}$$

3.2.3 The disposable soma model

Using above mentioned equations, the mathematical model incorporates the main ideas of disposable soma theory, such as maintenance, fertility and fitness.
In general, the model confirms the principles of disposable soma theory, which states that 'the organism should not waste resources by extending life span potential beyond what is likely to be seen in wild populations subject to external mortality'. *Kirkwood* and *Drenos* suggest that modeling disposable soma theory, survivorship *l(x)* can simply be increased by increasing investment in maintenance *s*. While the increase in fecundity *m(x)*, cannot

simply be achieved with increase in *s* and will lead to postponed maturity, diminishment of the peak reproductive rate and slowing of the age-related decline.

The model also predicts that there is a balance between growth and reproduction in one hand and maintenance on the other, and that increase in maintenance will lead to decrease in growth and reproduction.

3.3 Network theory of ageing

Another model purposed by *Kirkwood* and *Kowald* in 1995 integrates the contribution of defective mitochondria, aberrant proteins and free radicals as major players in the ageing process. Suggestions that ageing is result of multiple factors that work together formed the network theory of ageing. This fact would lead to greater predictive and explanatory capabilities then observations derived from a set of individual models. However, this approach makes many assumptions and simplifies some of the process in order to reconcile mathematical and biological complexity.

The model is also known as MARS model, which stands for **m**itochondria, **a**berrant proteins, **r**adicals, **s**cavengers (Figure3.3)

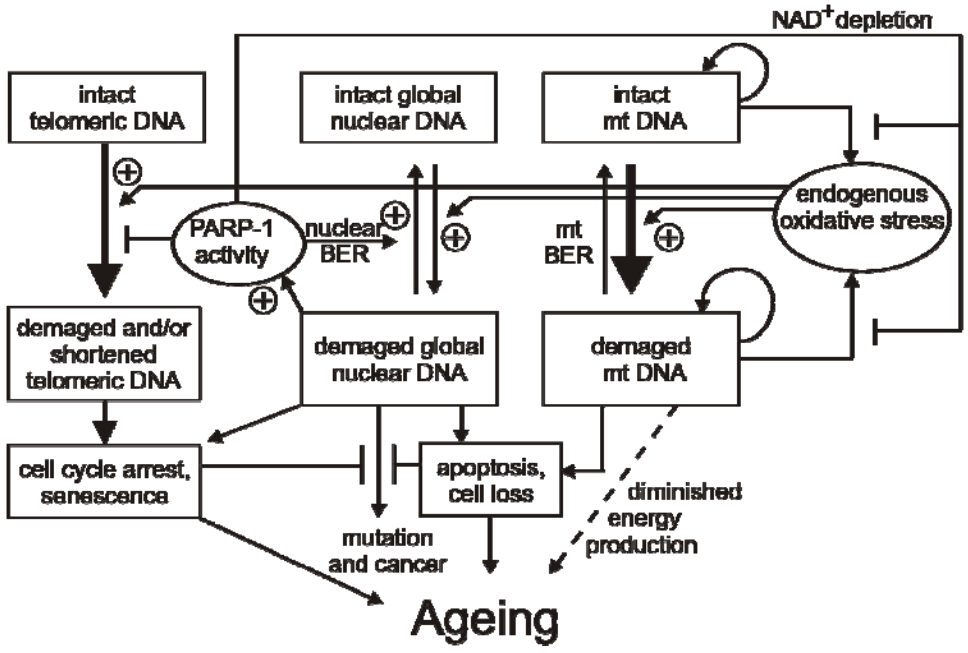

Figure3.3| Schematic representation of components of the MARS model. (adapted from Kowald A, Kirkwood TBL (1993))

The role of mitochondria is a central part of the model. Some of the functions modeled are mitochondria as ATP source, production of free radicals, mitochondrial replication and turnover. The fact that more radicals and less ATP are produced by damaged mitochondria is modeled trough different damaged classes. Various parameters describe different rates of mitochondrial replication, depending whether it is intact or damaged.

The second component of the MARS models is integrated in one and comprises of free radicals, aberrant proteins and antioxidants. A feedback loop controls the rate of synthesis of proteins and the assumption is that synthesis is regulated by product inhibition. Also, during protein synthesis, proteins can be damaged or their activity or specificity can be affected. Scavengers and antioxidants are regulated by substrate activation and the ribosomes by autoinhibition.

The full model consists of 35 differential equations and number of parameters. Such a large model generates a huge number of parameter combinations and simulations.

The MARS model explains the following observations and experimental findings:

1. the loss of specific enzyme activity; demonstrated by sharp increase of inactive proteins with age.
2. a decline in enzyme specificity
3. the significant increase in protein half-life with age
4. a decrease in mitochondria population with age
5. an increase of the fraction of mitochondria with age
6. an increase in the average rate of free radical production per mitochondria with age
7. a decrease in the average level of ATP generation per mitochondria with age

This method of *in silico* study of the extremely complex and important ageing process is the first attempt in generating an amalgamated model. It takes account the interactions between different processes and levels of function.

It is often a danger having complex models; due to inability to control the parameters or even worse validate any given hypothesis. Usually this type of models have a good fit to the data (they have many degrees of freedom). This is called the data *overfitting* and characteristic of these models is to have low predictive capabilities.

4. Mathematical Model of Accumulations of Damaged Proteins

To approach the questions, if there is an advantage of asymmetrical cell division – i.e. production of cells of different size, different levels of damage, and unequal reproductive potential, we developed a mathematical model aimed at elucidating effects of cellular asymmetries on fitness, proliferating capacity, and aging.

The mathematical model consists of a system of ordinary differential equations and a set of algebraic equations to describe how the accumulation of damaged proteins influences ageing in yeast. The model we propose has two main features. First, the set of ODEs describes the behavior of intact and damaged proteins through successive cell generations. Secondly, we define a set of rules for the distribution of proteins based on different modes of division and we introduce a retention coefficient that affects the distribution of proteins between progenitor and progeny.

4.1 Description of system dynamics in between two cell divisions

To simulate the proliferation of a simple entity consisting of two types of molecules (e.g. diffusible proteins), intact and damaged ones, we constructed a mathematical model based on ordinary differential equations (1). The ODEs describe the accumulation of the intact (P_{int}) and damaged (P_{dam}) proteins, such as oxidatively carbonylated proteins, during the cell cycle and successive cell generations. The sum (P) of intact (P_{int}) and damaged (P_{dam}) proteins determines the total size of the entity.

$$\frac{dP_{int}}{dt} = \frac{k_1}{k_s + P_{int} + P_{dam}} - k_2 P_{int} - k_3 P_{int}$$
$$\frac{dP_{dam}}{dt} = k_3 P_{int} - k_4 P_{dam} \qquad (4.1)$$
$$\frac{dP}{dt} = \frac{k_1}{k_s + P_{int} + P_{dam}} - k_2 P_{int} - k_4 P_{dam}$$

The temporal dynamics of intact proteins, P_{int} is given by a production term (maximal rate k_1) dependent on the current amount of total protein in the cell, the half-saturation term (rate constant k_s), a degradation term (rate constant k_2), and a term for the conversion of intact proteins into irreversibly damaged ones (rate constant k_3). The dynamics of damaged proteins P_{dam} is ruled by the conversion of intact proteins to damaged ones (k_3) and the degradation of damaged proteins (rate constant k_4).

Initially, the numbers of intact and damaged molecules increase until production and degradation is balanced, such that a steady state is approached (Figure 1A and B). Since protein and RNA synthesis in unicellular systems has been shown to increase either exponentially or pseudo-linearly during the cell cycle, we tested both types (linear and exponential) of cellular growth (Figure 4.1A and B), yielding comparable results when fitness, aging, and robustness were determined. Note that in the case of modelling exponential growth of the cell we multiplied the extra term P_{int} to the growth rate of intact proteins:

$$\frac{dP_{int}}{dt} = \frac{k_1 P_{int}}{k_s + P_{int} + P_{dam}} - k_2 P_{int} - k_3 P_{int} \qquad (4.2)$$

The protein production rate, k_1, has been adjusted by hand allowing for a steady state to be reached and has been assigned a final value of 10^7. We choose values of k_2 and k_4, the degradation rates of P_{int} and P_{dam}, respectively, so that $k_2 < k_4$. Degradation rates are

computed using the half-life formula $t_{1/2} = \ln 2/k$, where k is the degradation rate; setting the half-life of intact proteins to be 1 time unit, $k_2 = \ln 2$. Since degradation of damaged proteins is faster, k_4 needs to be greater than k_2 and it has been set to ln 5.

We also assumed all conversion of P_{int} to P_{dam} to be irreversible, such that no P_{dam} could be repaired back to P_{int}. To simulate different rates of conversion, k_3 has been given a range of values, from 0.1 to 2.3. Parameters were implemented to resemble known values describing cell growth, protein synthesis and degradation, accumulation of damage and its segregation.

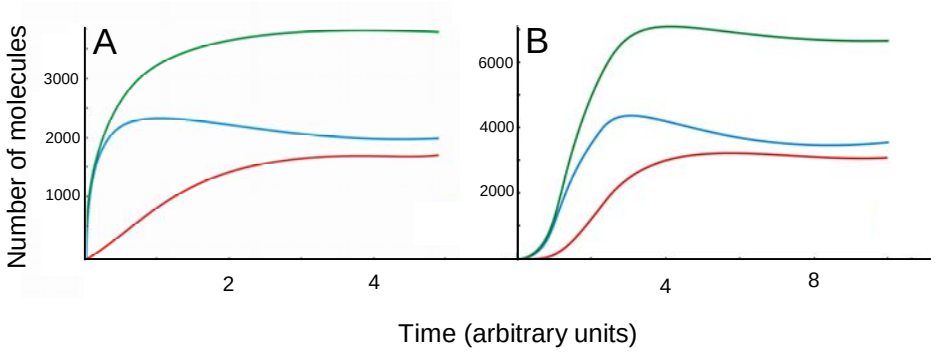

Figure4.1| Modeling linear and exponential growth of an entity consisting of intact and damaged proteins. Linear (A) and exponential (B) expansion of total (green), intact (blue) and damaged (red) proteins in a cell entity without division. The x-axes denote time (in arbitrary units), and the y-axes represent the amount of proteins (defined as the number of molecules/entity). Parameters values are $k_1=10^7$, $k_2=\ln 2$, $k_3=0.6$, $k_4=\ln 5$.

Note that in the simulation for the dividing entity shown later, most of the entities will never come close to this steady state, but remain in the initial phase of increasing protein concentrations.

4.2 Description of cell division

In the present model, cells initiate division once they have attained a critical cell size, defined by P_{int} reaching a value called P_{div}, arbitrarily assigned to 1500 molecules/cell in the present work. The following set of transition equations describes how the proteins are distributed between progenitor and progeny when the cells divide, i.e. when P_{div} is reached.

The subsequent equations are derived with following assumptions:

1. Total amount of proteins (P) in the cell would be sum of P_{int} and P_{dam}.
2. Sum of, the amounts of intact proteins in the progenitor and the amounts of intact proteins in progenies are constant before and after division. Similarly for damaged proteins.
3. Sum of the amounts of intact and the damaged proteins in the progenitor is constant. Similarly for progenies.

4.2.1 Without damage segregation

In the case of a protein distribution that is only dependent on size of the newly generated cells, the different cell types obtain the following amounts of proteins:

For progenitors:

$$\begin{aligned} P_{int}(g+1) &= P_{int}(g) \cdot s_{mother} \\ P_{dam}(g+1) &= P_{dam}(g) \cdot s_{mother} \\ P(g+1) &= P_{int}(g) \cdot s_{mother} + P_{dam}(g) \cdot s_{mother} \end{aligned} \tag{4.3}$$

For progenies:

$$\begin{aligned} P_{int}(g+1) &= P_{int}(g) \cdot s_{daughter} \\ P_{dam}(g+1) &= P_{dam}(g) \cdot s_{daughter} \\ P(g+1) &= P_{int}(g) \cdot s_{daughter} + P_{dam}(g) \cdot s_{daughter} \end{aligned} \quad (4.4)$$

The size of the progenitor, s_{mother}, denotes the percentage of protein from the previous generation that is kept in that cell, while the size of the progeny, $s_{daughter}$, expresses the percentage of protein assigned to the new-born cell. *P(g+1)* denotes the initial amount of total protein for the new generation *(g+1)*, while *P(g)* corresponds to the final protein amount before division of the previous generation *g* (similarly for P_{int}, P_{dam}).

4.2.2 With damage segregation

We next introduce a retention coefficient (*re*), describing the amount of P_{dam} being retained by the progenitor. In this case, segregation of P_{dam}, and consequently P_{int}, is affected by both size and retention, according to the following set of transition equations:

For progenitors:

$$\begin{aligned} P_{int}(g+1) &= P_{int}(g) \cdot s_{mother} - P_{dam}(g) \cdot re \cdot (1 - s_{mother}) \\ P_{dam}(g+1) &= P_{dam}(g) \cdot (s_{mother} + (1 - s_{mother}) \cdot re) \\ P(g+1) &= P_{int}(g) \cdot s_{mother} + P_{dam}(g) \cdot s_{mother} \end{aligned} \quad (4.5)$$

For progenies:

$$\begin{aligned} P_{int}(g+1) &= P_{int}(g)\cdot s_{daughter} + P_{dam}(g)\cdot s_{daughter}\cdot re \\ P_{dam}(g+1) &= P_{dam}(g)\cdot s_{daughter}\cdot(1-re) \\ P(g+1) &= P_{int}(g)\cdot s_{daughter} + P_{dam}(g)\cdot s_{daughter} \end{aligned} \quad (4.6)$$

When including the retention coefficient in the equations, the distribution of intact will depend on levels of damaged proteins, retention and size of the cell, due to the previously mentioned assumptions.

The maximum value for retention is $re = 1$, meaning that the progenitor keeps all damaged proteins, while for $re = 0$ the distribution of damage is proportional to the size of each cell, thus corresponding to a case without retention (see equations (4.3) and (4.4)). We simulated the model for various values of retention, ranging from 0.125 to 0.875 with a step increase of 0.125.

4. 2. 3 Size

To this end, we defined two different cell sizes, one for progenitors and one for progeny. We call the size of the progenitor s_{mother}, denoting the percentage of protein from the previous generation that is kept in that cell, also termed the mother cell. The size of the progeny is called $s_{daughter}$, giving the percentage of protein assigned to the new-born cell, now indicated as the daughter cell.

Upon symmetrical division, the size of both progeny and progenitor is equal, thus we have $s_{mother} = s_{daughter} = 0.5$ after division. After asymmetrical division, cells in the

next generation will have different sizes. We consider here the exemplary case that $s_{mother} = 0.75$ and $s_{daughter} = 0.25$.

Here, we give list of parameters used in our model.

Parameter	Description	Values	Assumptions
P_{div}	cell division threshold, in number of intact proteins	1500	size of the (mother) cell that triggers division
k_1	rate maximal protein production	10^7	adjusted by hand to allow steady-state
k_2	rate of degradation of intact proteins	ln2	half-life of 1 time unit
k_3	rate of damaging of intact proteins	[0.1,2.3]by 0.1	
k_4	rate of degradation of damaged proteins	ln5	half-life is shorter than for intact proteins, so $k_4 > k_2$
k_s	half-saturation constant	1	
re	retention coefficient	[0, 1] by 0.125	
s_{mother}	size of the progenitor after division	0.5 or 0.75	$s_{mother} + s_{daughter} = 1$
$s_{daughter}$	size of the progeny after division	o.5 or 0.25	$s_{mother} + s_{daughter} = 1$

Table 4.1|Parameters of the single-cell model, their default values and assumptions made

4.3 System Analysis

To study the potential of the model and understand the intertwined dynamics of cell division and protein accumulation through successive generations, we simulated the introduced equation systems for different cell sizes representing two types of divisions (symmetrical vs. asymmetrical), different damaged rates and different retention coefficients. In total we analyzed four different scenarios (Figure4.2 and Figure4.3) in detail:

1. Symmetrically dividing cells without retention
2. Symmetrically dividing cells with retention
3. Asymmetrically dividing cells without retention
4. Asymmetrically dividing cells with retention

In each scenario, we followed the fate of the progenitor and the progeny, separately, through a number of generations. We could thus draw a “mother lineage” and a “daughter lineage”, whereby we would, after every division, follow respectively the next generation of mothers only, or the next generations of daughters only.

All numerical simulations to follow individual time courses were carried out using Mathematica 5.2, Wolfram Research and SBML plug-in for Mathematica – SBMLMath.

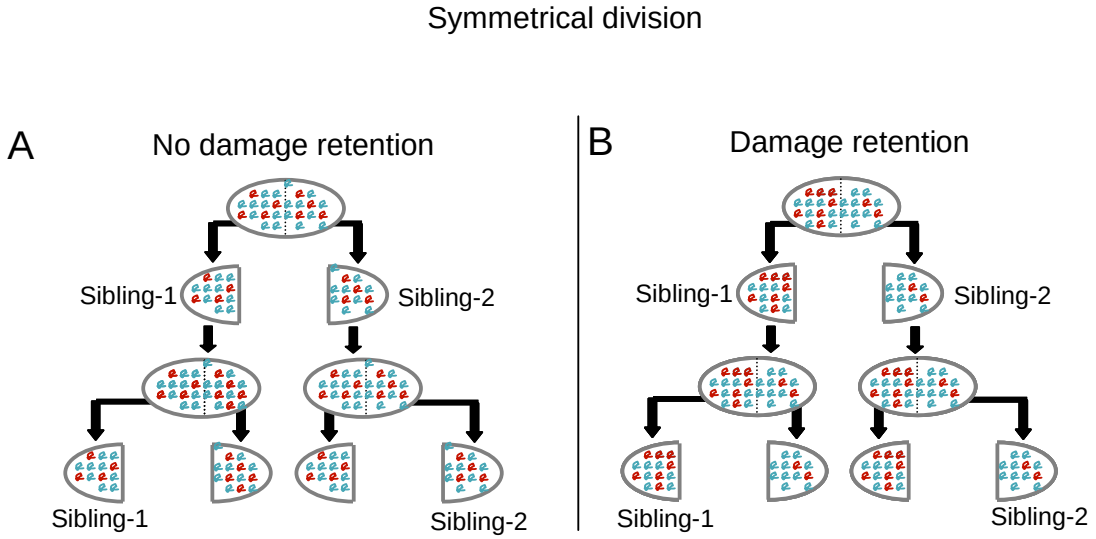

Figure 4.2|Symmetrically dividing system. Schematic representation of a symmetrically dividing system, the sibling lineages analyzed, and the distribution of intact (blue) and damaged (red) proteins in a system without (A) and with (B) damage segregation.

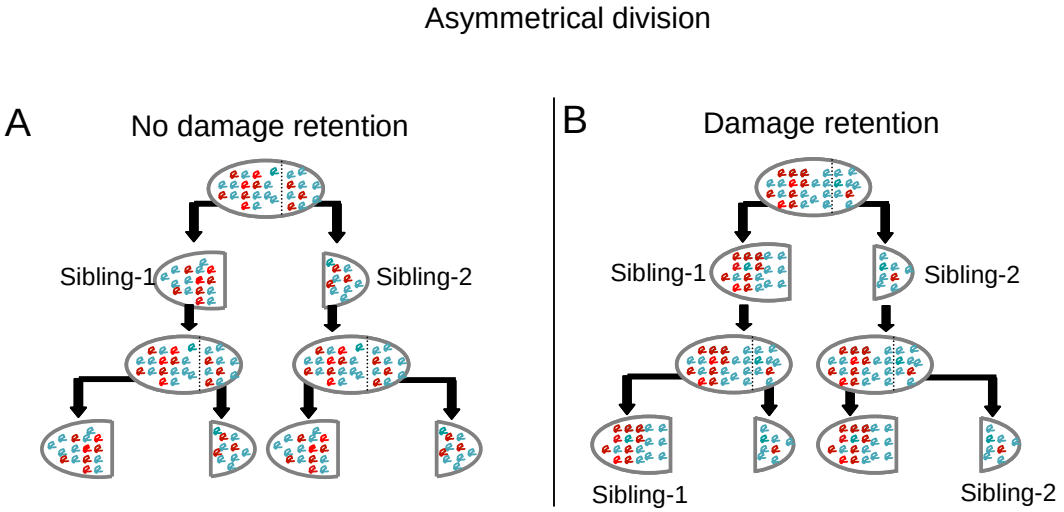

Figure 4.3|Asymmetrically dividing system. Schematic representation of an asymmetrically dividing system, the sibling analyzed, and the distribution of intact (blue) and damaged (red) proteins in a system without (A) and with (B) damage segregation.

4.4 Carbonilation study

Carbonilation levels in yeast cells can be obtained by a slot-blot procedure (Appendix C, section C.1). Protein extracts from cells are applied to the membranes; quantitative results from this type of experiment would give us the concentration of oxidatively damaged proteins per total.

To compare results attained from experimental study, with results from *in silico* study, for each cell cycle we calculated the amounts of damaged (P_{dam}) and total (P) proteins with the precision of 10 000 points per cell cycle, then the ratio of damaged to total proteins (P_{dam}/P) for each time point was calculated. The ratios are plotted as a function of time. See Appendix A, section A.3 for the complete simulation results, for asymmetric and symmetric cytokinesis, with and without segregation, for low, moderated and high damage rates.

Daughter's lineages for both types of division are starting a new generation time with lower P_{dam}/P ratio, then the mothers, and in each generation time the initial value for this ratio is the same as in the previous generation. The P_{dam}/P ratio is linearly increasing for each individual generation time, until it reaches the maximum value (point when the cell is dividing). In the case without retention, daughters will start with higher level of P_{dam}/P compared to the case when we have retention.

Mother's lineages P_{dam}/P ratio at the beginning of each generation time is higher then in the previous generation, showing linear increase. Damaged to total ratio within one generation time will decrease for very old mothers, while in the case of young once it will remain constant (initial and final value of P_{dam}/P within one generation time is almost the same).

4.5 Population study

In the previous section, the behavior of "mother lineages", i.e. the sequence of cells obtaining the larger share of volume for asymmetric division and the larger share of damaged proteins in case of retention; or "daughter lineages", consisting of cells always getting the smaller share was explored.

Based on the observation that populations consisting of symmetrically dividing cells with a low damage rate may live indefinitely, while populations with a higher damage rate will be completely extinct (all cell lineages are modeled to have the same fate), we may ask for evolutionary strategies that can help to ensure the survival of the population even at higher damage rates.

In order to estimate the fitness of the whole population, we calculated the population size for each scenario including the mixed lineages. To this end, we first derived the number of divisions per unit time, and then we combined the results from each type of lineage forming the population to obtain the corresponding size reached in a defined unit of time.
This way of calculating population is not very realistic, since we assumed that the generation times for each entity in the tree will be the same.
We wanted to get the rough estimated how the populations of cells, derived under different conditions, behave and to look at the evolutionary aspects of different strategies cell can acquire.

The population size was calculated (using a custom Perl-script (***www.perl.org***)) for each of the four scenarios previously mentioned, using different retention coefficients and different damage rates. For each pair (re, k_3), the number of cells produced per one time unit was calculated for both, mother lineage and daughter lineage. Then the tree consisting of those cells was constructed, where lineages would be edges of the tree. Afterwards, the mixed population was simply counted and would give estimates of the population size for a given pair. The data was plotted as size of the population (in the number of cells) *vs*. different damage rates (k_3).

Figure 4.14 (section 4.8.2) shows the interdependence of population size, damage rate and retention. Appendix A, section A.1 provides a summary of the quantitative results. For a detailed analysis and comparison we chose systems without retention and one with a retention coefficient of 0.875. All four scenarios are represented as a function of increasing damage (k_3) and were compared against each other.

4.6 Pedigree Analysis

The limitations in the simulations carried out with Mathematica didn't allow us to follow the fate of the mixed lineages.
To overcome the problems encountered with previous approach, we use a hierarchical model that allows us to explore any and all branches of the pedigree tree, and precisely track mother-daughter relations. We can therefore explore lineage specific properties, such as the rejuvenation property studied in this work.

4.6.1 BioRica system

BioRica is a high-level modeling framework integrating discrete and continuous multi-scale dynamics within the same semantic domain. It is in this precise sense of mixing different dynamics that BioRica models are *hybrid* following the classical definitions.

Moreover, BioRica models are built hierarchically. *Alur et al.* defined two types of hierarchy: *architectural* and *behavioral*. While Bio-Rica admits both, in the course of this work we are only concerned with the former. This type of hierarchy allows for both concurrency and parallel composition.

4.6.2 Building a hierarchical model

The hierarchical model we have defined explicitly tracks mother-daughter relations in pedigree trees of simulations. This thus allows us to study lineage-specific properties, which are properties associated with connected sub-graphs of the pedigree tree. In the pedigree tree, a given mother cell generates a series of daughter cells; these siblings are ordered in time, and the younger a sibling, the older the mother at the time of division.

A three-node hierarchical model was defined by adding a discrete controller above the quantitative single-cell model (Figure4.4). The BioRica platform was extended to take

account the new requirements for this study (see section 4.6.3, below). Simulation of this model generates pedigree trees of arbitrary depth.

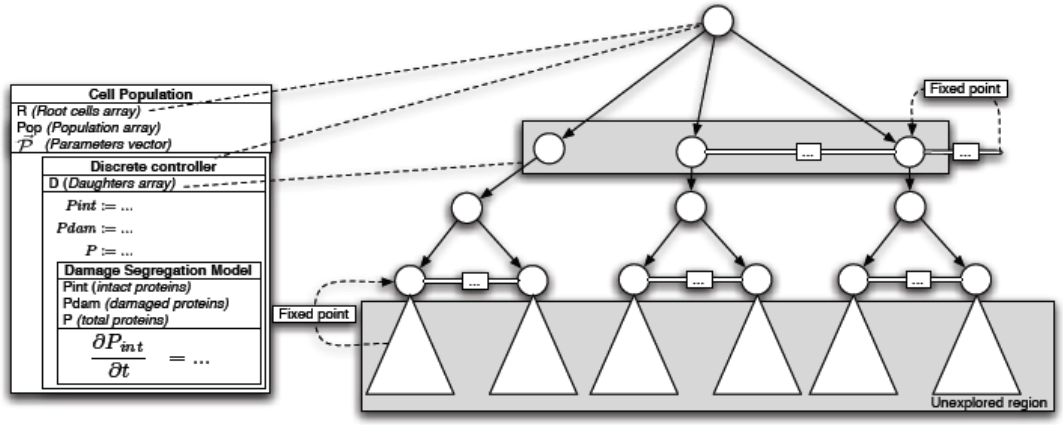

Figure4.4| Three level hierarchical model. The discrete cell population and cell division controllers and the continuous single-cell model. This model generates pedigree trees during simulation, instantiating new single-cell models for each cell division. Infinite width and depth are represented finitely by relaxing the tree constraints to permits loops from the leaves. These fixed points represent immortal cells or immortals lineages.

4.6.3 Adaptation of original algorithm

The original BioRica algorithm developed in the group of Macha Nikolski needed to be adapted for the damage segregation study (Appendix A). In particular, *alive* and *update* predicates had to be redefined in a specific way.

The *alive* predicate verifies three conditions:
First, the cell is checked for immortality, which is realized by the fixed point detection.
Second, we verify if the cell is in the state of clonal senescence: $P_{int}(S') > P_{int}(S)$.
Third, the condition on cell size is checked: $size < reP_{dam} / (P_{int} + reP_{dam})$.

The *update* has the role of managing the new cell creation. For the current cell *c* it updates its state variables according to the algebraic equations (4.3 - 4.6) and its statistics (fitness, generation time, etc). It creates a new cell node (daughter of *c*) according to the equations (4.3 – 4.6) and inserts it in the population array *Pop* (Figure4.5).

Algorithm 1 General simulation schema

Require: current state S, current simulation time t, maximal simulation time t_{max}

```
1:  S = S'
2:  while alive(S,S') = 1 and t < t_max do
3:      S = S'
4:      t, S =  advance numerical_integration()
5:     if e = discrete_events() then
6:        t = get discrete_event time()
7:        store_event(e)
8:        S = update(S, e)
9:        reset numerical integrator()
10:    end if
11:    store_state(S)
12:  end while
```

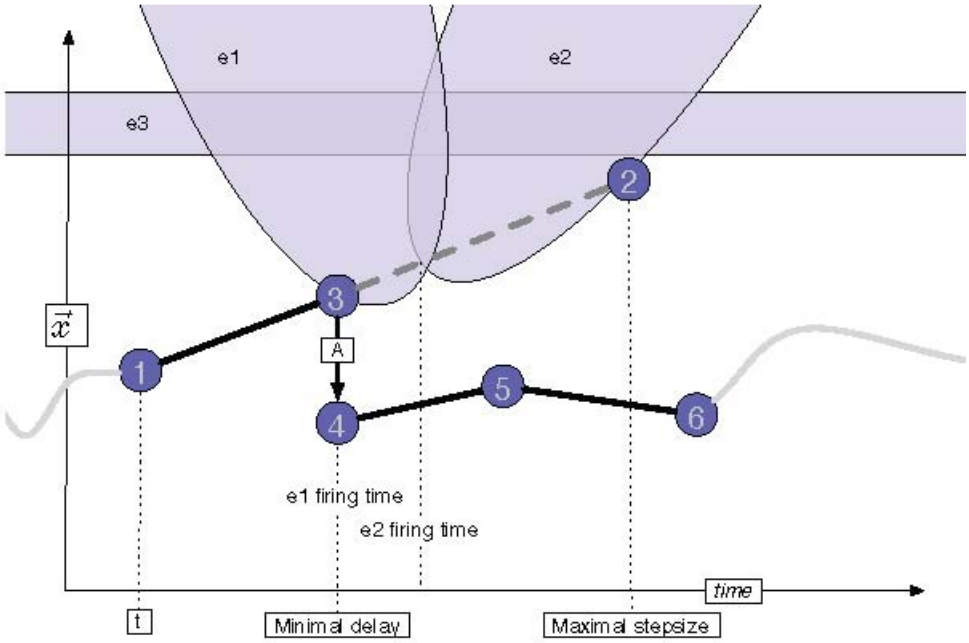

Figure 4.5| The algorithm. The numerical integrator advances between t (point 1) and the maximal step size (point 2). The guards of events e_1, e_2 are satisfied. The regions where these guards are satisfied are shaded. The firing time of e_1 (point 3) is used to reset the simulator after the discrete transition A (point 4).

4.6.4 Calibration of the system - simulation to depth 4

To calibrate and validate the system, complete simulations were run to depth 4 in the pedigree tree (representing all cells produced in the tree after a mother cell divided 4 times) for an exhaustive range of parameter values (Table 1 section 4.2.3). Rate constants k_1, k_2, and k_4 received fixed values; k_3 and re were given a range of values with small step sizes, and s_{mother} and were given $s_{daughter}$ two pairs of values representing symmetric and asymmetric growth strategies. A total of 625 simulations were run and stored in the pipeline database. Back-to-back comparisons with previous results were performed (ignoring pedigree) to validate the new simulator.

4.6.5 Pedigree exploration - simulation to depth 30

For each of the four scenarios studied here, a representative simulation was chosen by inspecting properties of the initial mother. From the whole parameter space, we selected simulations where the mother cell produces a number of daughters that is both finite and large enough (20-24 divisions depending on the case, since the average life span of wild type budding yeast is 24 divisions).

For each of these simulations, the pedigree tree was calculated up to depth 30, and for each cell in the tree we calculated five values: *initial damage* and *terminal damage* levels (corresponding respectively to the amounts of damage P_{dam} at the beginning of cell cycle, and at the end of the cycle when division is about to occur), *generation time* (time between two divisions), *absolute date of birth* (in arbitrary time units, measured from the moment when mother starts its first division) and the *fitness* (defined as number of divisions during first time unit).

4.7 Rejuvenation Study

Using parameter exploration we could identify sets of parameters that exhibit a given emerging high-level behavior. Moreover, the analysis of the emerging behavior can be done both at the single-cell and whole pedigree tree levels.

The model was analyzed for different initial amount of damaged and intact proteins. Thus, we could compute the critical level of terminal damage (P_{dam} at the point of division) to find the set of initial values which would gives us the cells that exhibit death (Figure 4.6 - left panel).

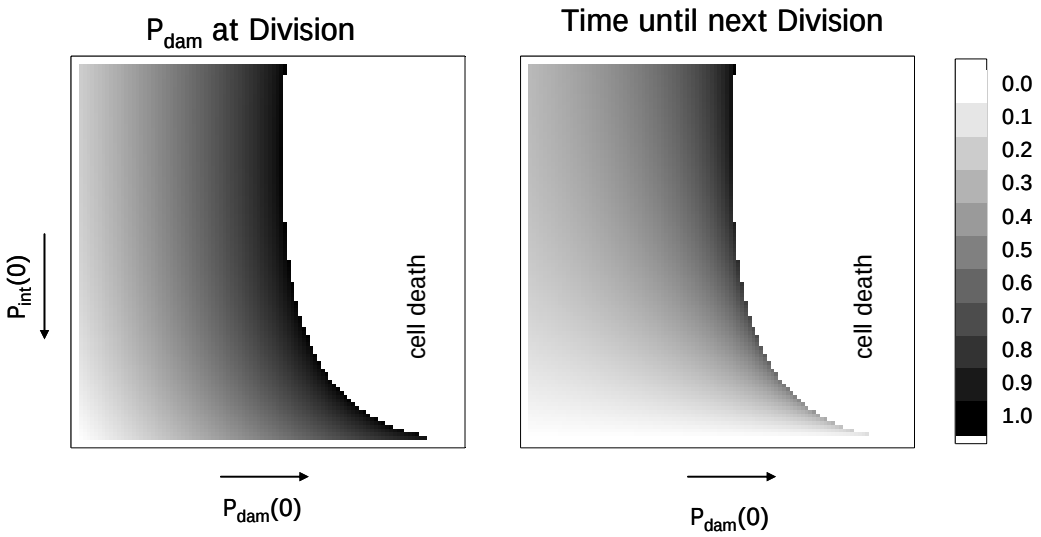

Figure 4.6| Variation of initial values of P_{int} and P_{dam} and their effect on terminal damage and generation time.

Similarly, the *time until next division* can be calculated as a function of initial values of intact and damaged proteins (Figure 4.6 - right panel).

However, here we observe the opposite effect of increased initial values of intact proteins, which lead to have long period of time until cell divides, which would correspond to long generation time and it is consistent with observations that generation time becomes progressively longer as mother cells become older.

We were interested in detecting cells that have a finite but high enough number of daughters (this would reflect the wild type cell of *S.cerevisia* with average life span of 24 divisions), and looking for parameters giving high rejuvenation value across the whole parameter space.

The hypothesis is that the rejuvenation will take place when the ratio of damaged and intact proteins at the point of division is lower then the same ratio at the beginning of the cell cycle (equation 4.7).

$$\frac{P_{dam}(t_{div})}{P_{int}(t_{div})} < \frac{P_{dam}(0)}{P_{int}(0)} \tag{4.7}$$

Thus, we could find the *rejuvenation line* (Figure 7) and *cell death line*, which would give us tree distinct areas*: rejuvenation*, *damage accumulation* and *cell death* area.

We can conclude that the rejuvenation effect depends on both protein species – intact and damaged ones. And that not all levels of intact proteins are prerequisite for rejuvenation. At low levels of P_{int}, damage can increase up to 60% of possible damage and the rejuvenation will still occur, beyond this point, if damage continues to increase the cell becomes dead. Otherwise, at high levels of intact proteins (more then 60%) the accumulation of damage will occur regardless of initial level of damaged proteins.

This would, then lead us to the conclusion that accumulation of damaged proteins would conflict with longer period before next division (Figure 4.6 – right panel and Figure 4.7 – left panel).

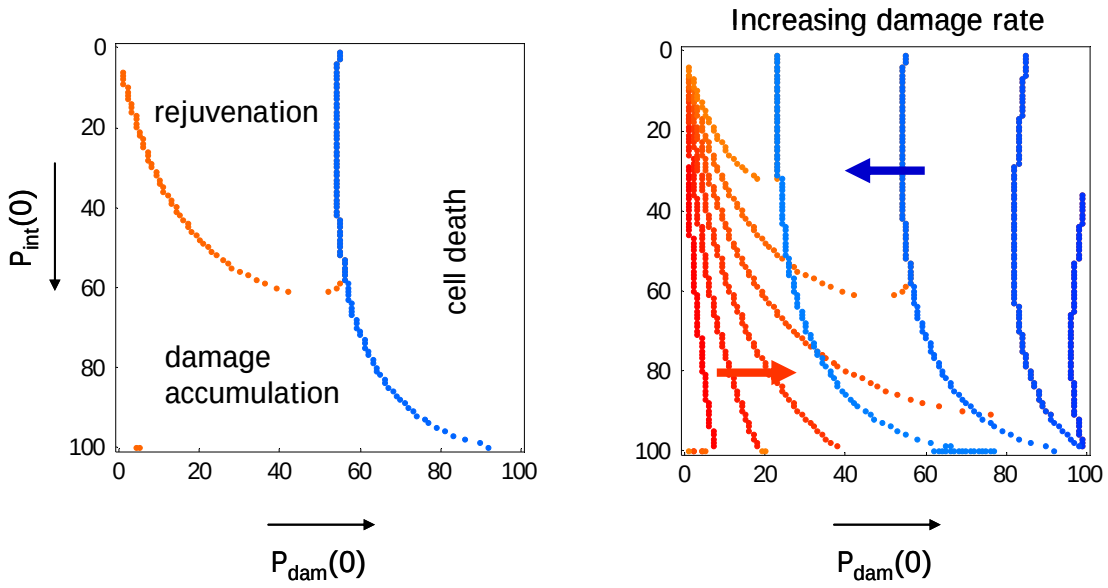

Figure 4.7| Theoretical approach to rejuvenation effect. The red lines divide areas of rejuvenation from areas where cells accumulate damage, depending on the initial amount of P_{int} and P_{dam}. The higher k_3, the *rejuvenation area* becomes smaller and *cell death area* larger (right panel)

4.8 Results

4.8.1 Effects of asymmetry on clonal senescence

With the equations at hand, we asked whether there is an intrinsic difference between symmetrically and asymmetrically dividing systems in their ability to cope with increasing rates of damage production. The model was simulated initially for low damage rates with an equal inheritance of damaged proteins (Figure 4.8A). Under these conditions the system is characterized by constant initial and final concentrations of intact and damaged proteins during successive generations and the population is immortal (Figure 4.8A). At moderate damage rates, cells still divide indefinitely but display longer generation times (Figure 4.8A). In contrast, at high damage rates, the cells go through a finite number of divisions characterized by progressively longer generation times and a pronounced accumulation of damaged proteins at the expense of intact ones, eventually preventing P_{div} from being attained (Figure 4.8A). Since division, in this simulation, is perfectly symmetrical and all cells in the population are identical, the outcome is clonal senescence. That is, the model predicts that at high damage rates the entire population eventually reaches a "dead end", reminiscent of the Hayflick limit.

We next asked whether a "division of labor", i.e. the unequal distribution of damaged proteins during cytokinesis (Figure 4.2B) among individuals affects the damage rate at which clonal senescence is reached. We therefore introduced the retention coefficient into the model (see equations (4.6) and (4.7)); such that equal-sized siblings are distinguishable by the amount of damaged proteins they inherit. The system now shows signs of sibling-specific replicative senescence, with the cells retaining more of the damage displaying progressively longer generation times whereas the "low-damage" sibling lineage propagates indefinitely (Figure 4.8B). In addition, everything else being equal, damage segregation (Figure 4.8B) allows the population to expand at damage rates, which cause clonal senescence of a perfectly symmetric system (Figure 4.8A).

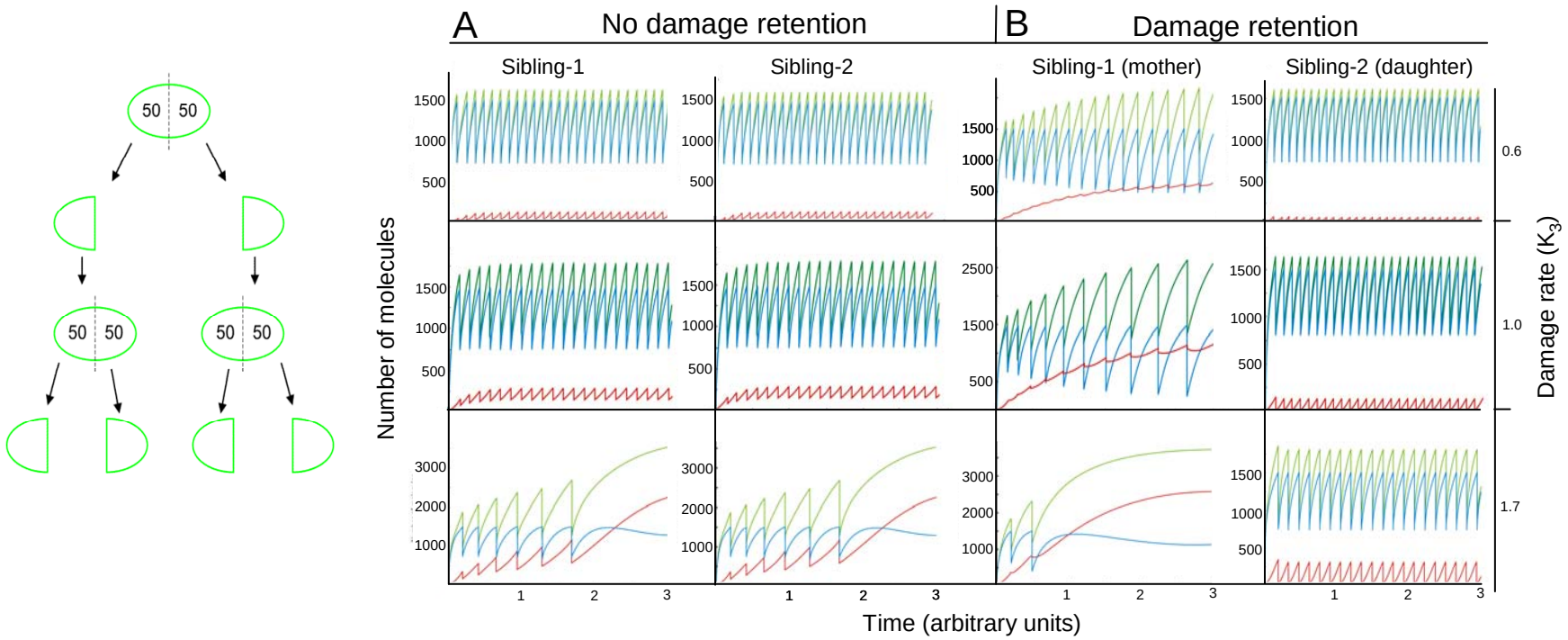

Figure4.8| Symmetrical division.Time course comparison between symmetrically dividing cells without retention and with retention of damaged proteins and with a low, medium and high degree of damaged proteins being generated. We see that all three protein amounts P, P_{int}, P_{dam}, increase until P_{int} reaches P_{div}. Then the cells divide and distribute protein amounts according to equations (4.3) and (4.4) in case of no segregation or equation (4.5) and (4.6) in case of segregation. Mother and daughter cells, in the case of symmetrical division we would refer to them as sibling-1 and sibling-2 behave identically when division is symmetric and retention not applied (Figure2A); however, they follow two distinct patterns of protein inheritance, when retention is introduced (Figure 2B).

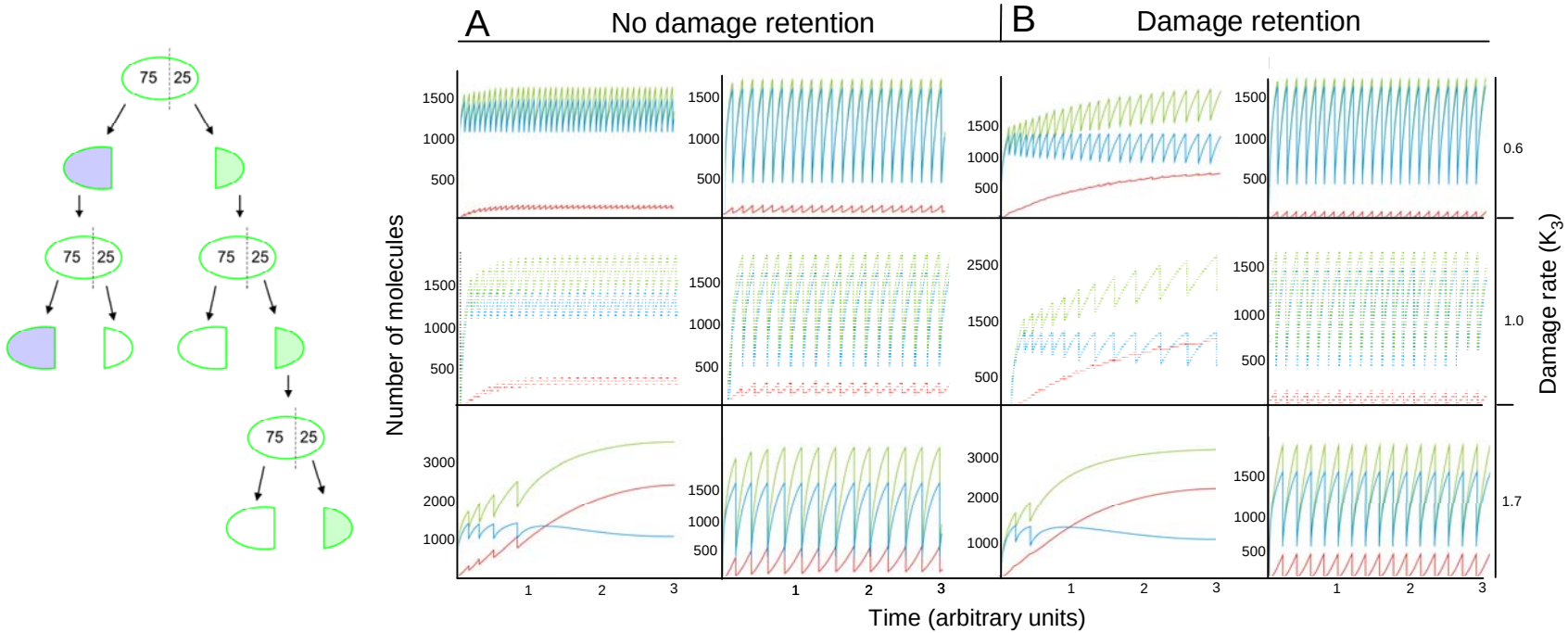

Figure4.9| Asymmetrical division. Time course comparison between asymmetrically dividing cells without retention and with retention of damaged proteins and with a low, medium and high degree of damaged proteins being generated. We see that all three protein amounts P, P_{int}, P_{dam}, increase until P_{int} reaches P_{div}. Then the cells divide and distribute protein amounts according to equations (4.3) and (4.4) in case of no segregation or equation (4.5) and (4.6) in case of segregation. In the case of no segregation, protein distribution is only dictated by size and therefore mother cells (corresponding to 75% of the common cell entity before division) will reach the trigger faster than daughters and hence produce more divisions/unit time than the latter.

This analysis was followed by testing whether a difference in size alone between a large progenitor and a smaller offspring (Figure 4.3A) is sufficient to prevent clonal senescence. In this context, the inheritance of intact and damaged proteins is proportional to the relative size of each cell entity at division. At low to moderate damage, the system now shows signs of a sibling-specific replicative senescence, typical of asymmetrical dividing systems, such as budding yeast. The larger parent lineage (mother cell) displays increasingly longer generation times (Figure 4.9A) until eventually the persistent titration of intact proteins by damaged ones prevents it from dividing again. In contrast, at the same damage rate, the smaller progeny lineage continues to divide indefinitely (Figure 4.9A). Also, a system of different-sized progeny can expand *ad infinitum* even without damage segregation at damage rates giving rise to clonal senescence in the perfectly symmetrical system (Figure 4.8A and 4.9A). When damage was segregated such that the larger mother cells received an even higher load than expected from its size (Figure 4.9B), the system could withstand even higher levels of damage before clonal senescence commenced (Figure 4.9B).

The model also suggests that in order to prevent clonal senescence the degree of damage segregation (or size asymmetry) needs to increase as the damage production rate is elevated (Figure 4.10A and B). The trade-off for this beneficial effect of damage retention or size asymmetry on clonal senescence is sibling-specific aging at progressively lower damage rates (Figure 4.10A and B). Interestingly, even very low retention coefficients (re=0.125; one sibling effectively retaining 58% of the overall P_{dam}) are sufficient to prevent a symmetrically dividing population from reaching a “dead end” at moderate damage rates (Figure 4.10A).

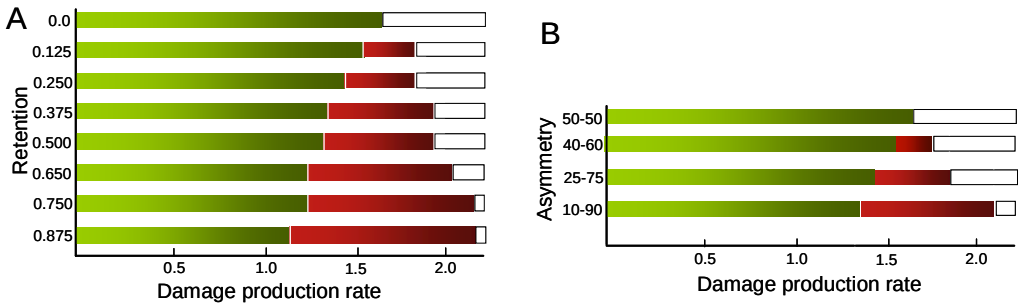

Figure 4.10| Damage segregation and size asymmetry causes sibling-specific aging but increases the robustness of the system. (A) Effect of damage segregation (y-axis) on damage levels (k_3; x-axis) triggering clonal senescence and replicative aging. Green bars indicate that both siblings produced during cytokinesis are immortal but exhibit longer generation times with increasing damage. Red bars indicate that the sibling retaining more damage at the time of cytokinesis undergoes replicative senescence, i.e. can only perform a finite number of new generations, whereas the other sibling is immortal. Empty bars indicate that the system has reached clonal senescence, i.e. a damage rate at which both siblings display a finite ability to produce new cells. (B) Effect of size asymmetry (y-axis) on damage levels (k_3; x-axis) triggering clonal senescence and replicative aging. Color-coding is as described in "A".

4.8.1.1 Generation time

The simulations also suggest that the generation time of the damaged-enriched mother cell increases exponentially with each cell division in the system displaying damage retention whereas a slow linear increase is observed for mother cells without retention of damage (Figure4.11A). Again, the experimental data for mother cells of budding yeast fits best with the simulations of damage retention (Figure4.11B).

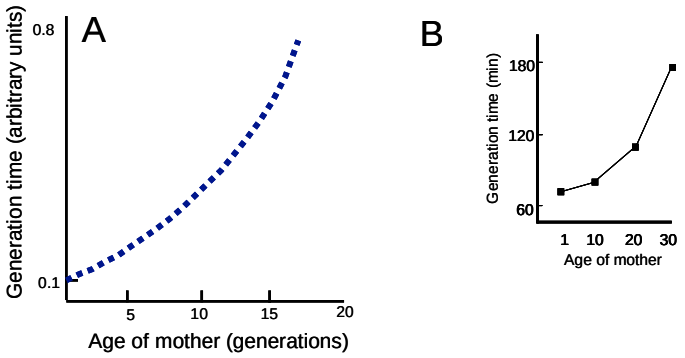

Figure4.11| Effect of damage segregation on generation time of the mother-cell lineage in an asymmetrically dividing system. (A) Changes in generation time (y-axis) are plotted as a function of age of the large mother cell in an asymmetrically dividing systems without (red) and with (blue) damage segregation. (B) Experimental data for the generation time of yeast mother cells as a function of the replicative age.

4.8.1.2 Increase in size

One of the biomarkers for yeast ageing process is increase in size. This is, probably, the most obvious feature of a senescent cell. Several studies showed that the volume of the yeast cell increases linearly with age and that the senescent cell can be four times as large as an exponentially growing cell.

A system obeying the roles of P_{div} and damage propagation as stipulated in the equations requires that the mother cell becomes progressively larger with each division, which is

seen experimentally for yeast mother cells. This is true for simulations of systems both with and without damage segregation and the differences are too small to use as a predictive factor for experimental results (Figure4.12). However, the simulations suggest that a virgin daughter cell of a budding yeast (asymmetrical system) needs to acquire a larger size before initiating cytokinesis if damage is not segregated; this is exactly what is observed in *sir2* mutant daughter cells, which, on average, are 40% larger than wt daughter cells at the time of cytokinesis and display a 2-fold higher load of damaged proteins.

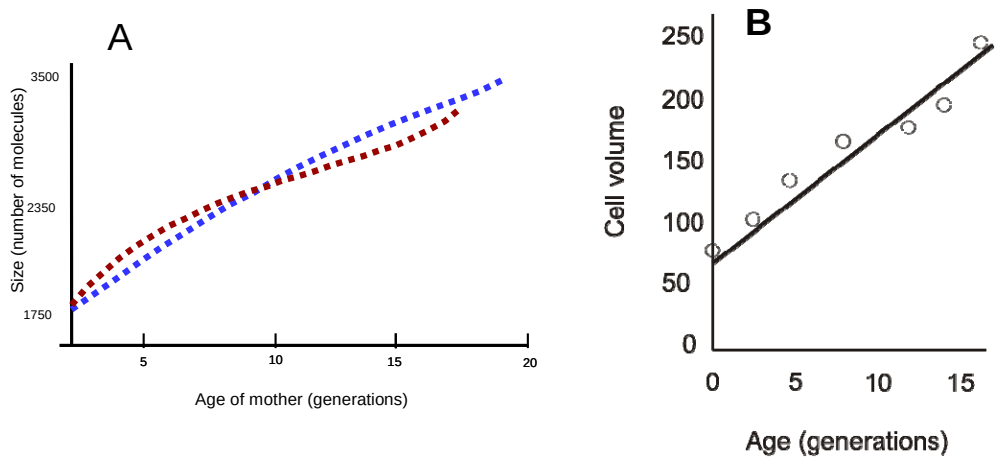

Figure4.12| Effect of damage segregation on size of the mother-cell lineage in an asymmetrically dividing system. (A) Changes in size (y-axis) are plotted as a function of age of the large mother cell in an asymmetrically dividing systems without (red) and with (blue) damage segregation. (B) Experimental data for the volume change of yeast mother cells as a function of the replicative age (adapted from *Egilmez et al, 1990)*

4.8.1.3 Carbonilation levels

The asymmetrically dividing yeast, *S. cerevisiae,* is known to segregate damage. Using the model, we tested how such segregation is predicted to affect the progressive accumulation of damage in the aging mother cells. As depicted in Figure 4.13A, damage segregation accelerates the accumulation of damage in aging mother cells and results in a

differential accumulation of damage during the cell cycle – mother cells that retain damage have longer generation times and the number of damaged molecules (per total) is somewhat decreasing during the cell cycle (Figure 4.13A). In contrast, mother cells that do not retain damage exhibit more even levels of damage throughout the cell cycle and do not display the step-wise increase in damage upon cytokinesis observed in damage-retaining mother cells (Figure 4.13A). We measured the concentration of oxidatively damage proteins (per total) in synchronized yeast mother cells during two successive divisions and noted that the damage displays a step-wise increase in the mother cell upon completion of cytokinesis (Figure 4.13B).

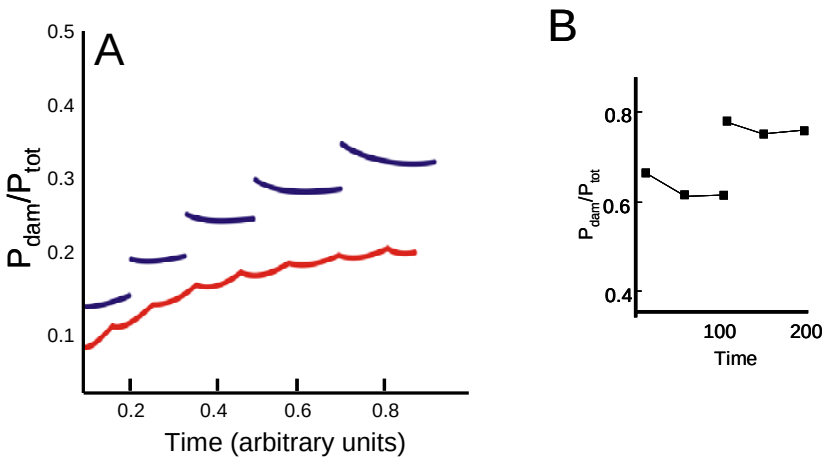

Figure4.13| Effect of damage segregation on damage accumulation of the mother-cell lineage in an asymmetrically dividing system. (A) The ratio of damaged to total number of molecules (y-axes) in the large mother cells during progressive cell cycles in an asymmetrically dividing system without (red) and with (blue) damage segregation. In the system without retention, the large mother cells accomplish 7 divisions and the system with retention 4 divisions during the time shown. (B) Experimental data for the ratio of oxidized to total proteins during two successive cell cycles of yeast mother cells: an asymmetrical system known to segregate damaged proteins.

4.8.2 Effects of asymmetry on population fitness

While the model suggests that asymmetrical systems can withstand higher degrees of damage before entering into clonal senescence, it does not necessarily mean that asymmetrical systems display an increased fitness or evolutionary advantage. If we define fitness as the number of entities produced, in total, per time unit, the population fitness of the different systems can be calculated at different damage production rates. When doing so for a system that divides symmetrically size-wise, damage segregation surprisingly improves population fitness at all damage rates analyzed (Figure 4.14A). Thus, the model predicts that damage segregation may be favored irrespective of the degree of damage in a system dividing by binary fission. A similar conclusion, at one fixed damage level, was reached by Ackerman et al. and Watve and al. who described the effects of differentiation between an aging parent and rejuvenated offspring in a population of unicellular organisms.

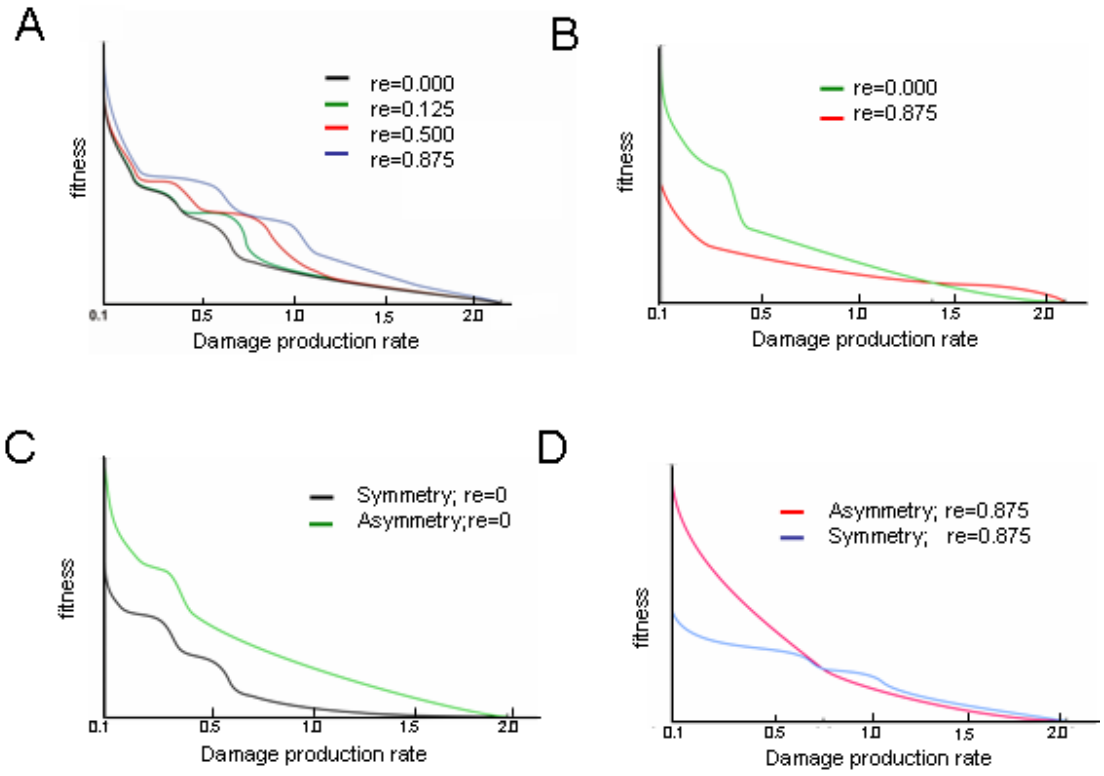

Figure4.14| Effects of asymmetries on population fitness upon increasing rates of damage production. Fitness, defined by the population size produced within one time unit (y-axis), is plotted as a function of increasing damage rate (k_3; x-axis). The different retention coefficients modelled are color-coded and shown in the graph. (A) Fitness of symmetrically dividing systems (by size) displaying different degrees of damage segregation as indicated. (B) Fitness of an asymmetrically dividing system (by size) displaying no retention (green) and retention (red). (C) Fitness of a symmetrically dividing system without damage retention (black) compared to an asymmetrically dividing system without damage retention (green). (D) Fitness of a symmetrically dividing system with damage retention (blue) and an asymmetrically dividing system with the same degree of damage retention (red)

In contrast, in a system with different-sized progeny, damage partitioning, based on the model and assumptions made, is only beneficial at high damage propagation rates (Figure 4.14B). On the other hand, a population dividing asymmetrically will present a substantial fitness advantage over one dividing symmetrically at all damage rates (Figure 4.14C). However, if damage is segregated, an asymmetrical system is favored at low damage but looses out at high damage (Figure 4.14D). This can be explained by the fact that larger parent cells will reach the size for division (P_{div}) much faster than their symmetrically dividing counterparts (Figure 4.8 and 4.9). The fact that the smaller progeny have a longer generation time does not outweigh the parents' rate as long as the proportion of intact constituents is sufficiently high. However, as the damage rate increases, the progenitor lineage slows down, making the fitness largely dependent on the smaller offspring. At this point, the beneficial effect of retention allows a symmetrically dividing population with retention to be equally well off, or overtake, an asymmetrically propagating one (Figure 4.14D).

4.8.3 Damage segregation in a system dividing by binary fission

Segregation of damage has, so far, only been demonstrated for the asymmetrically dividing budding yeast. The fact that our simulations suggest that a system dividing symmetrically by size is more robust (withstand more damage before reaching clonal senescence) and displays an increased fitness at all damage propagation rates when partitioning its damage during cytokinesis raises the possibility that damage segregation is more common than previously anticipated and occurs also in cells dividing by binary fission. This prompted us to analyze the in situ distribution of carbonylated proteins in the fission yeast, *Schizosaccharomyces pombe*.

While the volume of the two siblings is equal, previous landmarks of division (birth scars), will remain confined to one half of the growing cell and be inherited by one "sib" only (Figure 4.15). When following birth scars and protein carbonyls during the cell cycle in synchronized cells, we found that carbonylated proteins display a discrete and dynamic localization within the cell (Figure 4.16). Quantification of carbonyls demonstrated that damage is inherited asymmetrically between the two siblings such that the one with the previous birth scar always retains the largest load of the damage (Figure 4.16). After completion of cytokinesis, the newborn cells display most of their damage at the new end (Figure4.16).

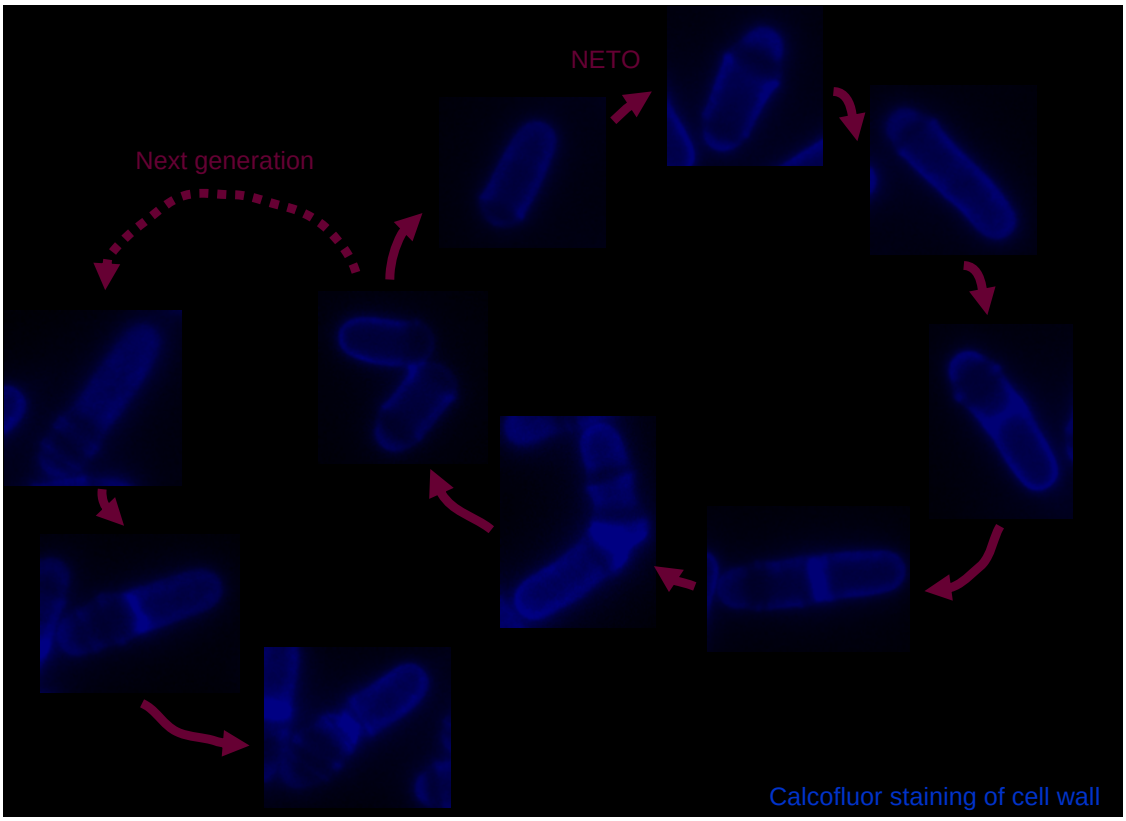

Figure4.15| *S.pombe* progression through cell cycle. Localization of septum and birth scar(s), visualized with calcofluor white, in cells of *S. pombe* during progression through the cell cycle.

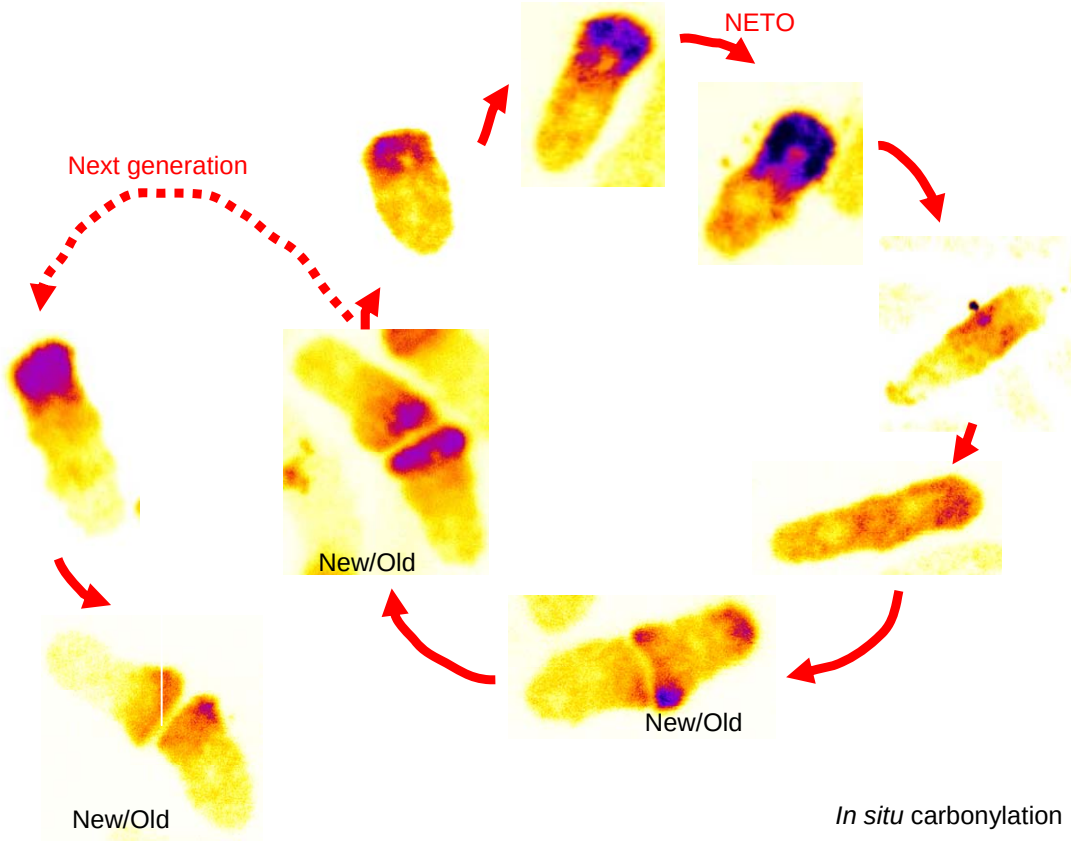

Figure4.16| Damaged proteins are asymmetrically segregated during binary fission of *S. pombe.* Distribution of carbonylated proteins during the cell cycle. Blue/purple denotes the highest concentration of carbonyls followed by red and yellow.

We next investigated whether partitioning of damaged proteins between the two siblings correlated with differential fitness or longevity. We followed the replicative potential of both sibling lineages, arising from division of a common parent cell, which had already completed 9 divisions and thus accumulated damaged proteins (see Figure 4.17A). We found that the sibling enriched for birth scars and protein damage ("old" sib) displayed a shorter mean life span (12.5 generations) than the "young" sib (15.9 generations)(Figure 4.17B), Moreover, the generation time of the damage enriched cell was markedly longer – 4.5 hours compared to 2.5 hours for the new sib (Figure 4.17C). This result points to a "sibling-specific" aging in *S. pombe* that correlates with the unequal inheritance of damaged proteins.

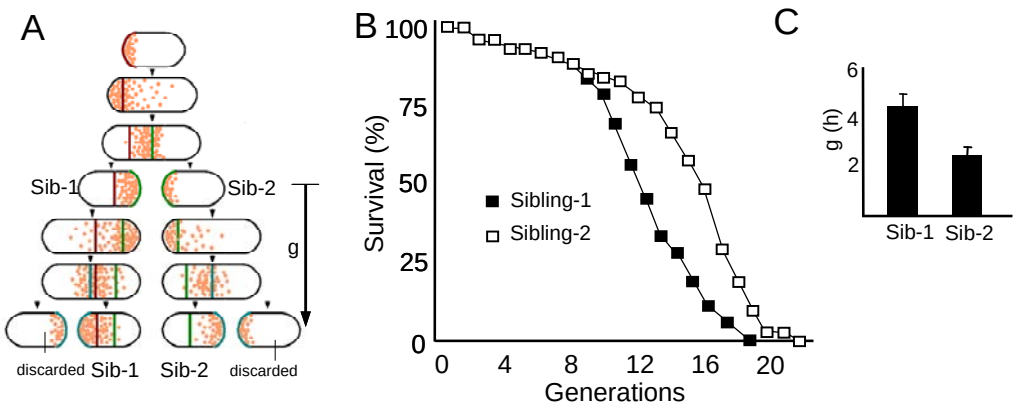

Figure4.17| S. pombe display sibling-lineage specific aging. (A) Schematic representation of the criteria used in discriminating between "old" (Sib-1) and "new" (Sib-2) sibling, derived from a common 9 generations old progenitor (starting cell). Vertical bars indicate birth scars, present as bulges on the cell surface, and here represented chronologically by different colors. Upon division, the cell with more birth scars (= more divisions) and rounder appearance was selected as the "older" sibling. These cells coincide with those inheriting more carbonylated proteins, as detected by immunofluorescence microscopy and here depicted by orange dots. (B) Replicative life span of the "old" sibling (Sibling-1; closed squares; n=75), and "new" sibling (Sibling-2; open squares; n=75) derived from a common 9 generations old progenitor cell. (C) Generation times for "old" (Sib-1) and "new" (Sib-2) sibling.

4.8.4 Pedigree analysis

In the pedigree tree, a given mother cell generates a series of daughter cells: these siblings are ordered in time and the younger a sibling, the older the mother at the time of division. (Figure 4.18)

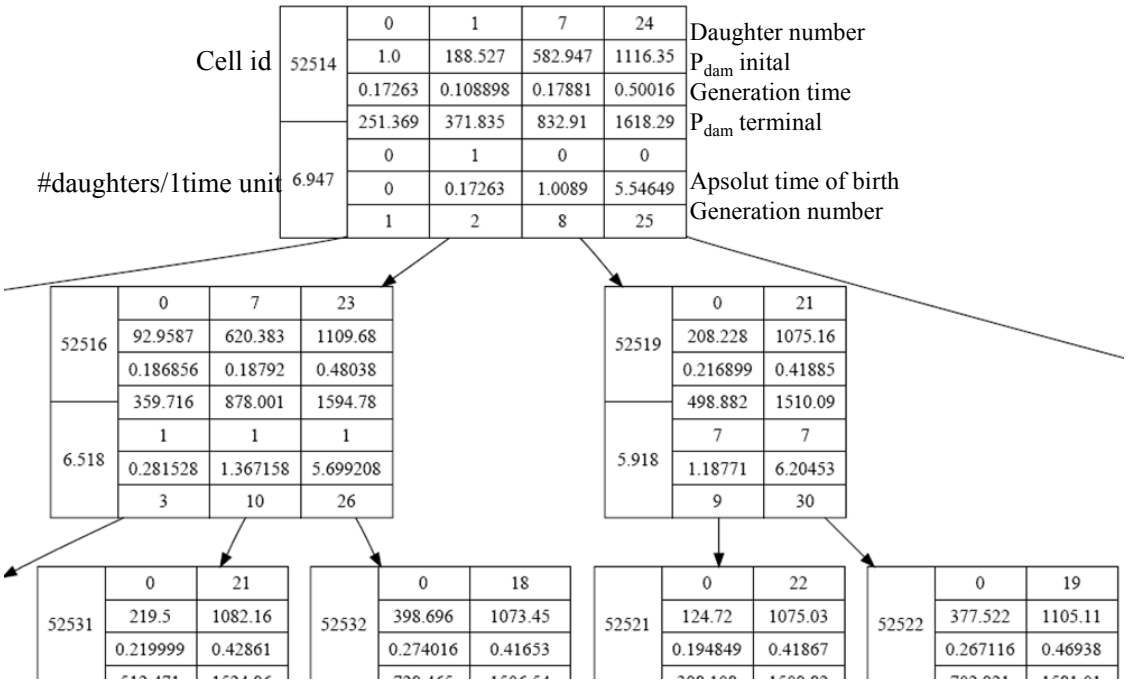

Figure4.18| Extract of typical pedigree tree. Full tree is in Appendix A, section A.4.

In the pedigree tree, the root represents the mother cell with following information: *Daughter number* – daughter reproduced by the root cell, P_{dam} *initial* – amount of damaged proteins at the beginning of the cell cycle for given daughter, *Generation time* – the length of the cell cycle for given daughter, P_{dam} *terminal* - amount of damaged proteins at the end of the cell cycle for given daughter, *Absolute time of birth* – cumulative time of birth counted from the fist daughter produced, *Generation number* – depth of the tree developed for specific mother The second level of the tree represents grand daughters of root mother, third level are grand-grand daughters, and so one.

Analyzing the pedigree trees obtained from BioRica simulator can be hard since the generated trees are usually very large and overwhelmed with all kinds of information, we can extract data of interest for specific phenomena and generate simplified trees. Example of such a tree, made for capturing the behavior of damaged proteins at the point of cell division (end of cell cycle) for a successive daughter cells is shown below (Figure 4.19).

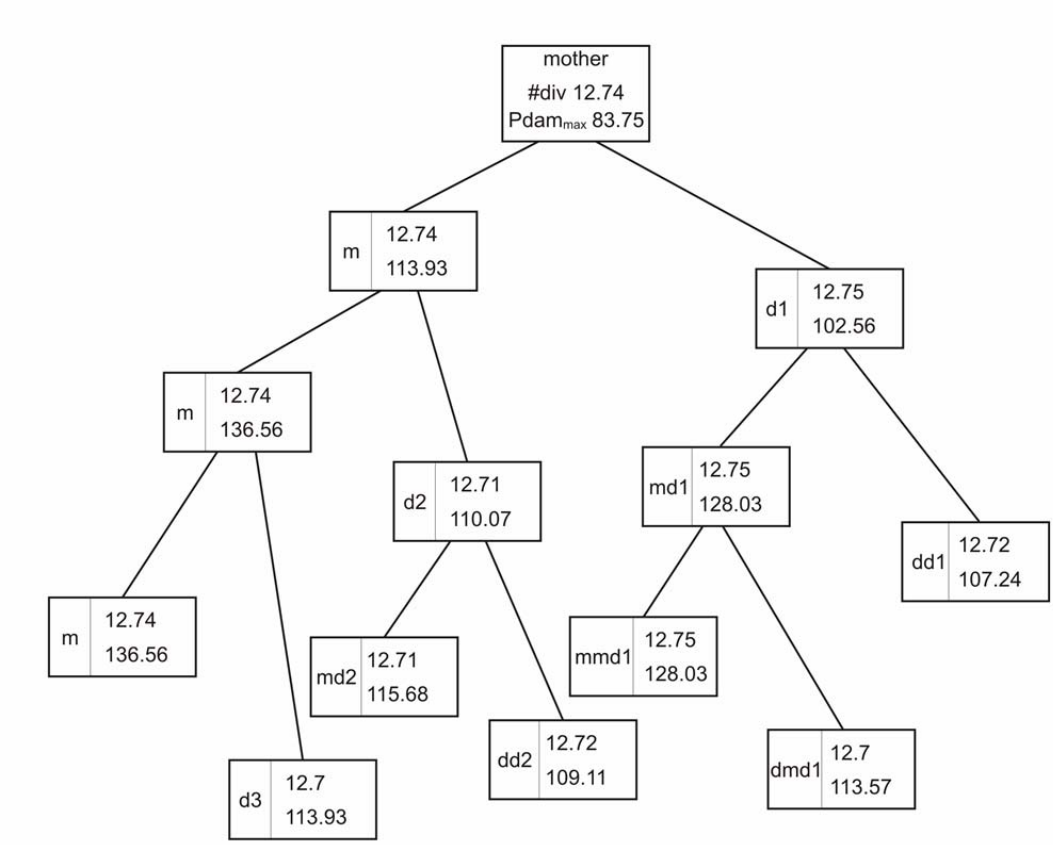

Figure 4.19| Simplified pedigree tree. The mother – daughter relationship is presented, showing only fitness and terminal damage amount. m- mother, d_i – i^{th} daughter, md*i* - i^{th} daughter becoming the mother, dd_i – i^{th} daughters daughter, dmd_i – i^{th} daughter of mother obtained from i^{th} daughter.

We observe in simulation results that younger siblings have higher damage, consistent with inheritance from an older mother that has accumulated more damaged proteins, and these younger siblings are thus born "prematurely old." This increase in damage accumulation is reflected in the decrease of fitness values (Figure 4.19).

4.8.5 Rejuvenation

Extending analysis of the pedigree tree, one level further, we can obtain grand-daughters cell line (second generation). We observed that daughters born early to the same mother have low damage, and their daughters have normal fitness. Daughters born late to the same mother have high damage and lower fitness, but remarkably, in asymmetric division with or without retention, their own daughters are born with lower damage and higher fitness (Figure 4.20 and 4.21)

This increase in fitness in the second generation is a *rejuvenation effect*, in part explaining how populations maintain viability over time despite inheritance of protein damage. The testable hypothesis is thus that there exists a mechanism for retention of damaged proteins during cell division, that attenuates the accumulation of such proteins in descendants, and that a combination of the precise value of the corresponding retention coefficient (*re*) and the asymmetry coefficients (s_{mother} and $s_{daughter}$) in the model determines the scale of the rejuvenation effect. These predictions are consistent with in vivo experimental results reported in the literature: *Kennedy* (1994) reported that daughter cells of an old mother cell are born prematurely old, with lower replicative potential, but that the daughters of these daughters have normal life spans. It should therefore be possible to experimentally estimate the value of the retention coefficient through indirect measures of cell lifespan and replicative potential.

As a control, we also inspected the case of symmetric division without damage segregation (Figure 4.22). We would not expect a rejuvenation effect, since inheritance of damaged proteins should be proportional in both mother and daughter cells, and indeed this is what is observed.

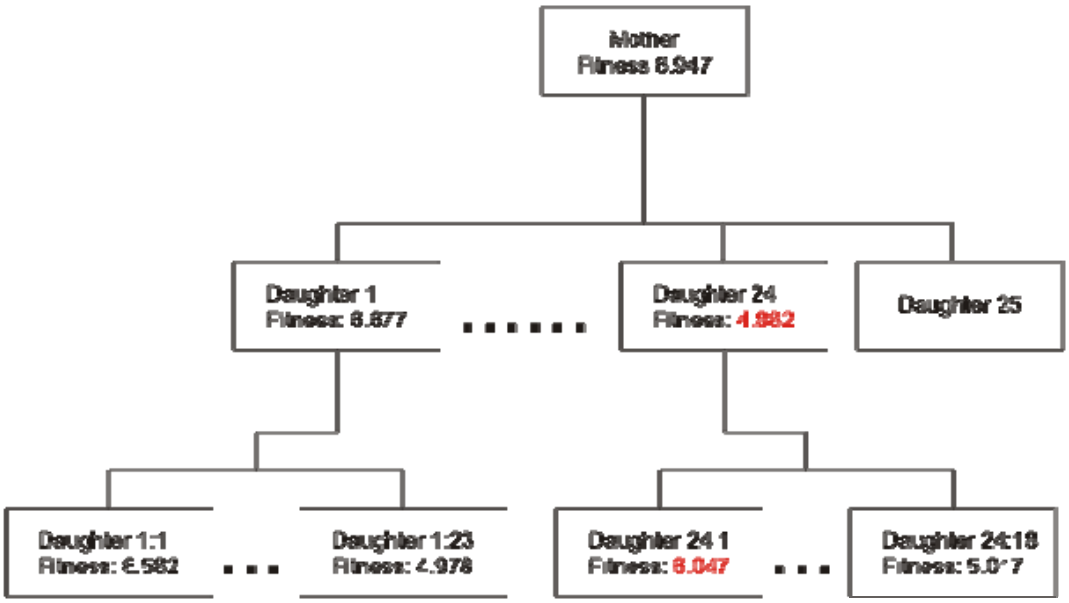

Figure 4.20| Asymmetrical division without retention. Mother cell is represented in the root of the tree, in the second level all her daughters are given (this particular mother produces 25 daughters before dying). In the third level, daughters produced by daughter 1 and daughter 24 are presented. Fitness is calculated as the number of cells produced per time unit. In the second level the fitness decreases as mother's age increases. The *rejuvenation* effect is seen in the third level of the tree, where the first daughter produced from 24th daughter (in the second level) has increased fitness.

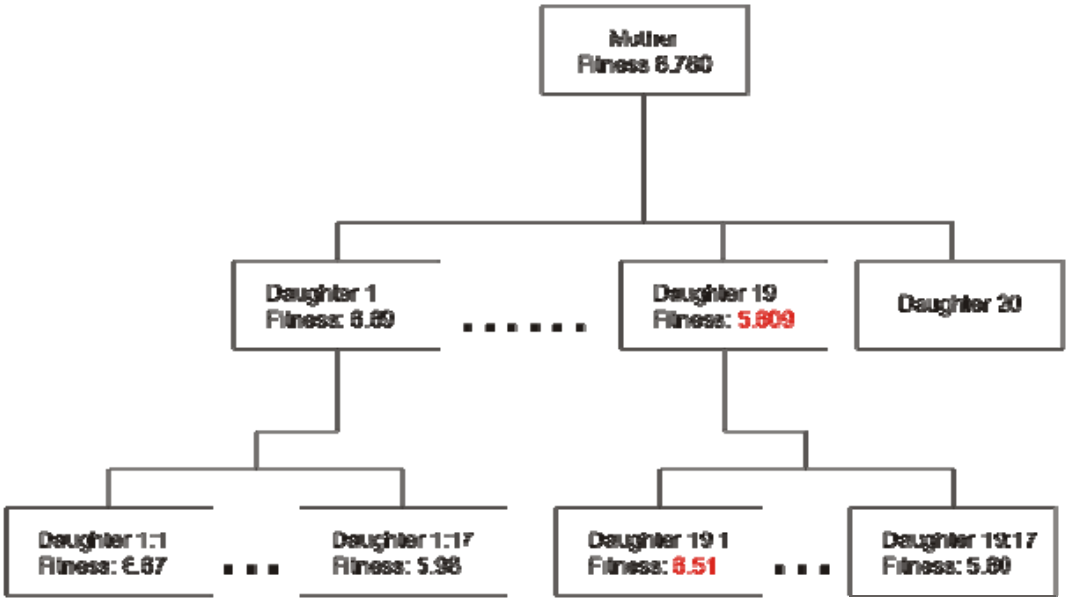

Figure 4.21|Asymmetrical division with retention. Mother cell is represented in the root of the tree, in the second level all her daughters are given (this particular mother produces 20 daughters before dying). In the third level, daughters produced by daughter 1 and daughter 19 are presented. Fitness is calculated as the number of cells produced per time unit. In the second level the fitness decreases as mother's age increases. The *rejuvenation* effect is seen in the third level of the tree, where the first daughter produced from 19th daughter (in the second level) has increased fitness.

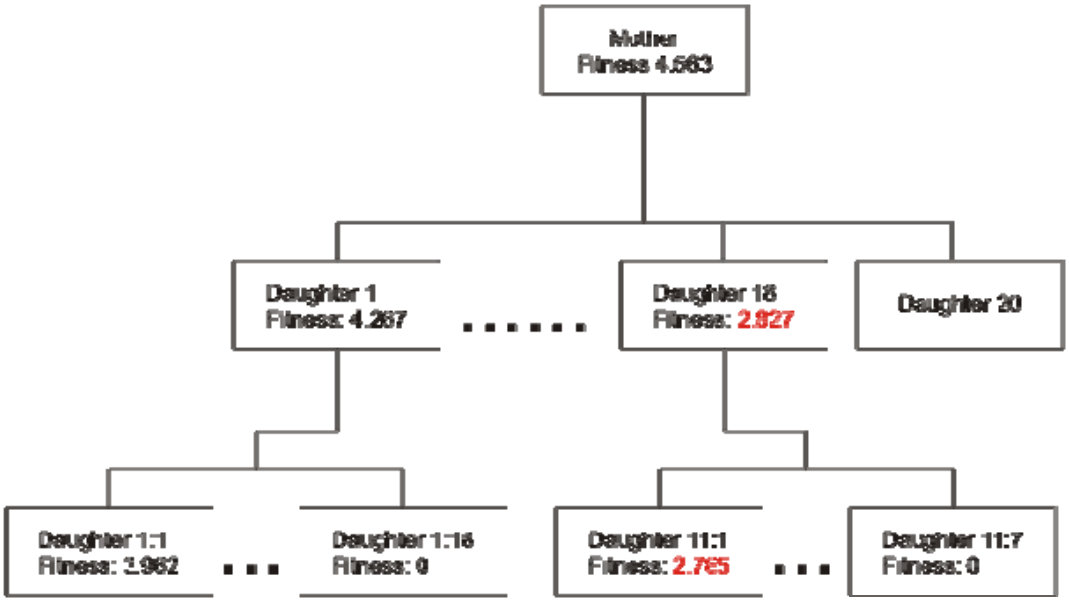

Figure4.22| Symmetrical division without retention. Mother cell is represented in the root of the tree, in the second level all her daughters are given (this particular mother produces 20 daughters before dying). In the third level, daughters produced by daughter 1 and daughter 18 are presented. Fitness is calculated as the number of cells produced per time unit. In the second level the fitness decreases as mother's age increases. Since the division is perfectly symmetrical *rejuvenation effect*, as expected, is not observed.

4.8.6 Sensitivity Analysis

Division threshold (P_{div}) – the amount of intact proteins that cell has to attain before division, can in theoretical approach mimic the various cell sizes critical for division. This can be used to simulate different mutants whose size is either smaller or larger then in the wild-type cells. Keeping all the parameters as before, we can decrease P_{div} as low as 1 molecule, and increase it up to 3500 molecules (at this threshold the system will not divide – we call this maximum size of the cell). As the level of P_{div} is decreasing, the number of divisions per one unit time will exponentially increase for all cells regardless of the division type. And, as we increase P_{div}, the number of division per one time unit will exponentially decrease. To verify the robustness of the system, the population size was obtained for both types of division, without retention and with retention (re=0.875). The results are showing the same trend and behavior as for the P_{div}=1500. The only difference is that the bigger the P_{div}, the lower damage system can handle (maximum damage is k_3=1.2).

Increasing the rate of degradation of damaged proteins (k_4), such that $k_2 < k_4$, we will get daughters that will never reach clonal senescence, while their mothers will be able to cope with higher damage (k_3). Higher rate of degradation for intact proteins ($k_2 > k_4$) will affect fitness of mothers and daughters and their capability of handling higher damage rates. Both, mothers and daughters will reach clonal senescence much earlier (k_3=0.7).

Finally, in simulations we observe that fitness and viability are sensitive to precise values of k_3, the rate by which proteins are damaged. This provides a series of testable hypotheses that could be investigated experimentally in different damaging environments, such as oxidative damage or radiation damage.

5 Discussion

Despite the large number of experimental data, the full understanding of complex ageing process is still unknown. The natural way would lead to development of mathematical models which would serve as a platform for better understanding of produced data, would allow integration of diverse information and postulate untested scenarios. With the instruments developed in the field of systems biology, tackling such issues become more feasible and realistic.

This work represents the first dynamic ageing model and further more a model applicable to different species. Previous models were mainly stochastic (formation of ERCs developed by Gillespie, bacterial ageing model developed by Ackermann) or more general and very descriptive and not suitable for direct experimental comparison (disposable soma model and MARS model, both developed by Tom Kirkwood).

In the this work we approached the questions of whether there is an advantage to producing daughter cells of different size, different loads of damage, and unequal reproductive potential. We investigated the impact of damage accumulation on population robustness and fitness and tested different strategies through which the effects of damage can be ameliorated. The models predicts that in a growing system adhering to the rules and assumptions made, there is a maximum amount of damage the cell system can tolerate, beyond which the proportion of intact constituents becomes insufficient for the cell to carry out any further division. In a completely homogeneous population, this point is marked by the simultaneous death (growth-arrest) of all individuals, i.e. clonal senescence (Figure 4.2A). The entities of the population could, of course, avoid such clonal senescence by reducing the rate of conversion of intact proteins to damaged ones (k_3) or increasing the rate of damage protein removal (k_4), i.e. by increasing their investment in classical maintenance pathways. However, the simulations suggest that there are other means of "rescuing" a cell population having reached clonal senescence, mainly by diversifying individuals within the population. This can be achieved either by

unequal partitioning of damage during cytokinesis or producing progeny of different size. In either case, this diversification of individuals leads to lineage-specific aging. This is in line with views of *Partridge* and *Barton* (1993) and *Kirkwood* (1981), who considered potential benefits of asymmetry in simple unicellular systems and how this might develop into aging.

The uneven distribution of damaged proteins may seem intuitive for organisms displaying markedly asymmetrical cytokinesis such as budding yeast; less so when there is no apparent distinction between the two sister cells. However, *Stewart* and colleagues demonstrated that *Escherichia coli* cells enriched with old pole material displayed a longer generation time than their new pole enriched siblings, indicating asymmetries also in systems dividing by binary fission. Although the measured differences in generation times are small in absolute terms, such asymmetry may be of significance for the robustness and fitness of the population. Our model suggests that even very low retention coefficients, e.g. a scenario where one cell receives 58% and the other 42% of the damage, may have a great impact on the systems ability to escape clonal senescence, at least at moderate damage rates (Figure 4.10). As the damage rate increases, the damage retention, or size asymmetry, needs to be more pronounced to allow the survival of the population.

However, when the total fitness (number of cells produced per time unit) of the systems is considered, damage retention may be a mixed blessing; for example, when considering a different cell-size organism like budding yeast, damage retention will push the upper limits for how much damage the system can endure before entering clonal senescence (Figure 4.10) but become a selective disadvantage at low damage production rates (Figure 4.14). This raises the question of whether the efficiency of damage segregation could be adjusted with changing environmental demands. Interestingly, damage segregation in budding yeast becomes more pronounced following increased oxidative stress, suggesting that this unicellular organism, indeed, enjoys the capacity to increase damage segregation upon conditions elevating such damage. In addition, unusually difficult growth conditions elicit a switch from a morphologically symmetrical to a more

asymmetrical type of division in fission yeast indicating that also this organism display a dynamic ability to break up symmetry upon environmental demands.

One common assumption in reports modeling potential benefits of asymmetry is that the establishment of age asymmetry is linked to damage segregation. However, such segregation of damage has, as far as we know, only been shown in the asymmetrically dividing budding yeast and one of the somewhat surprising predictions of the model presented here is that a system dividing symmetrically by size (binary fission) display a higher fitness if damage is segregated regardless of the damage accumulation rate. This suggests that damage retention may be more common than previously anticipated and prompted us to analyze the distribution of oxidatively carbonylated proteins during cytokinesis in the fission yeast *S. pombe.* We show that *S.pombe* displays an uneven distribution of carbonylated proteins between siblings, which correlates with their longevity and fitness (Figure 4.15, 4.16 and 4.17). This result can explain why growth in the presence of minor stressors results in a higher mortality of the "sibs" with more birth scars, i.e. the ones shown here to inherit more damage. Even though partitioning of damaged proteins to the "older" sib is not as pronounced as that of the budding yeast, it appears to be sufficient to entrust the "younger" sib with a significantly longer replicative potential and shorter generation time (Figure 4.17). As stated above, our modeling approach predicts exactly this, i.e. that a small bias towards damage asymmetry has profound consequences on the population's fitness and propagation. Our experimental results suggest that damage asymmetry is a purely random and stochastic phenomenon. In addition, the inheritance of the major load of carbonylated proteins is always coincident with the cell displaying more birth scars.

In summary, within the constrains of the equations and the assumptions made, the data suggests that both damage and size asymmetries pushes the upper limit for how much damage a self-propagating unicellular system can tolerate before entering clonal senescence. We believe the data raises the possibility that *sibling-specific* aging and *rejuvenation* in unicellular systems may have evolved as *by-products* of a strong selection for damage segregation during cytokinesis. A question of interest is whether such

division of labor between cells undergoing division is retained also in multicellular organisms, for example during the generation of germ line cells or differentiation.

This thesis showed that computational modeling poses considerable challenges at both theoretical and experimental levels. The model we developed is yet simple, but fully predictive, which, as stated at the beginning of this work, is the main feature a model should have. As a first step ageing model confirmed the findings of well studied model organism – *S.cerevisiae* (changes in size, generation time and damage load), then showed the importance of having damage segregation mechanism to ensure the immortal population. Finally, the model predicted the damage segregation on symmetrically dividing system – *S.pombe*, which was not previously anticipated. This led us to conclusion that asymmetrical damage distribution is one of the key factors in ageing organism and that immortal populations are not specific to size-wise asymmetrically dividing systems.

.

References

http://www.sanger.ac.uk/PostGenomics/S_pombe/docs/nurse_lab_manual.pdf

http://www.sbml.org

http://www.wolfram.com/

http://www.r-project.org/

http://www.perl.com/

http://www.yeastgenome.org/

Abrams PA, Ludwig D (1995) Optimality Theory, Gompertz' Law, and the Disposable Soma Theory of Senescence, Evolution, Vol. 49, No. 6, pp. 1055-1066

Ackerman M, Chao L, Bergstrom CT, Doebeli M (2007) On the evolutionary origin of aging. Aging Cell 6, 235-244

Ackermann M, Stearns SC, Jenal, U (2003) Senescence in a bacterium with asymmetric division. Science 300, 1920.

Aguilaniu H, Gustafsson L, Rigoulet M, Nyström T (2003) Asymmetric inheritance of oxidatively damaged proteins during cytokinesis. Science 299, 1751-1753.

Antal T et al., (2007) Aging and immortality in a cell proliferation model, Journal of Theoretical Biology 248, 411–417

Austad SN (1997) Why We Age. New York: John Wiley and Sons

Austriaco NR. (1996) Review: to bud until death: the genetics of ageing in the yeast *Saccharomyces*. Yeast 12: 623-630

Barker MG, Walmsley RM. (1999) Replicative ageing in the fission yeast Schizosaccharomyces pombe. Yeast. 15:1511–1518

Beckman, KB, Ames, BN (1998) The free radical theory of aging matures. Physiol. Rev. 78, 547-581.

Bitterman KJ, Medvedik O, Sinclair DA. (2003)Longevity regulation in *Saccharomyces cerevisiae*: linking metabolism, genome stability, and heterochromatin. Microbiol. Mol. Biol. Rev.67:376–399

Bruggeman FJ, Westerhoff HV (2007) The nature of systems biology, Trends Microbiol 15, pp. 45–50

Cacuci, DG, Ionescu-Bujor M, Navon M, (2005) Sensitivity And Uncertainty Analysis: Applications to Large-Scale Systems *(Volume II)*, Chapman & Hall.

Chakravarti B, Chakravarti D (2007) Oxidative Modification of Proteins: Age-Related Changes, Gerontology,53:128-139

Drenos F, Kirkwood TBL (2005) Modelling the disposable soma theory of ageing. Mechanisms of Ageing and Development, 126, 99-103.

Egilmez NK, Jazwinski SH (1989) Evidence for the involvement of a cytoplasmic factor in the aging of the yeast *Saccharomyces cerevisiae*. J Bacteriol 171: 37−42

Egilmez NK, Chen JB, Jazwinski SM (1990) Preparation and partial characterization of old yeast cells. J Gerontology 45:B9-B17

Elliott SG, McLaughlin CS (1978) Rate of macromolecular synthesis through the cell cycle of the yeast *Saccharomyces cerevisiae*. Proc. Natl. Acad. Sci. USA 75, 4384-4388.

Erjavec N (2007) Divide et impera: damage segregation and rejuvenation in yeast, PhD thesis, Göteborg University, Sweden

Erjavec N, Nyström T (2007) Sir2p-dependent protein segregation gives rise to a superior reactive oxygen species management in the progeny of *Saccharomyces cerevisiae*. Proc. Natl. Acad. Sci. USA 104, 10877-10881.

Erjavec N, Nyström T (2007) Sir2p-dependent protein segregation gives rise to a superior reactive oxygen species management in the progeny of *Saccharomyces cerevisiae*. Proc. Natl. Acad. Sci. USA 104, 10877-10881.

Evans S, Steinsaltz D (2007) Damage segregation at fissioning may increase growth rates: A superprocess model, Theoretical Population BiologyVolume 71, Issue 4, pp.473-490

Fabrizio P, Longo VD (2003) The chronological life span of *Saccharomyces cerevisiae*. Aging Cell. 2:73–81

Fantes PA (1982) Dependency relations between events in mitosis in *Schizosaccharomyces pombe*. J. Cell Sci. 55, 383-402.

Farout L, Friguet B, Proteasome (2006) Function in Ageing and oxidative stress: implication in protein maintenance failure, Antioxidants & Redox Signaling. 8(1-2): 205-216. doi:10.1089/ars.2006.8.205

Freeman-Cook LL. et al. (2005) Conserved locus-specific silencing functions of *Schizosaccharomyces pombe sir2*$^{+}$. Genetics 169, 1243-1260.

Friguet B, Bulteau A-L, Chondrogianni N, Conconi M, Petropoulos I, (2000) Protein Degradation bt the proteasome and its implication in ageing, Annals of the New York Academy of Sciences, 908:143-154

Gavrilov LA, Gavrilova NS (2001) The reliability theory of aging and longevity, J. Theor. Biol. 213, pp. 527–545

Gillespie CS, Proctor CJ, Boys RJ, Shanley DP, Wilkinson DJ, Kirkwood TB, (2004) A mathematical model of ageing in yeast, J. Theor. Biol. 229, pp. 189–196

Gillespie DT (1976) A General Method for Numerically Simulating the Stochastic Time Evolution of Coupled Chemical Reactions, Journal of Computational Physics 22(4), 403-434

Gillespie DT (1977) Exact Stochastic Simulation of Coupled Chemical Reactions, The Journal of Physical Chemistry, Vol. 81, No. 25, pp. 2340-2361

Gillespie JH (1974) Natural selection for within-generation variance in offspring number, Genetics 76, pp. 601–606

Glynn JM, Lustig RJ, Berlin A, Chang F. (2001) Role of bud6p and tea1p in the interaction between actin and microtubules for the establishment of cell polarity in fission yeast. Curr Biol. 11(11):836-45

Grune, T, Jung, T, Merker, K, Davies, KJA (2004) Decreased proteolysis caused by protein aggregates, inclusion bodies, plaques, lipofuscin, ceroid, and 'aggresomes' during oxidative stress, aging, and disease. Int. J. Biochem. Cell Biol. 36, 2519-2530.

Guarente L (2000) Sir2 links chromatin silencing, metabolism, and aging. Genes Dev. 14, 1021-1026.

Hamilton W D (1966) The moulding of senescence by natural selection. J. Theor. Biol. **12**:12-45

Harman D (1981) The aging process. In: Proc. Natl. Acad. Sci. USA 78, pp. 7124–7128.

Hayflick L, Moorhead P (1961) The serial cultivation of human diploid cell strains. Exp. Cell Res. 25, 585-621.

Hernebring M, Brolen G, Aguilaniu H, Semb H, Nyström T (2006) Elimination of damaged proteins during differentiation of embryonic stem cells. Proc. Nat. Acad. Sci. USA 103, 7700-7705.

Holliday R. and Kirkwood, TBL (1981) Predictions of the somatic mutation and mortalization theories of cellular ageing are contrary to experimental observations. J. Theor. Biol. 93, pp. 627–642

Holliday, R (1975) Growth and death of diploid and transformed human fibroblasts. Fed. Proc 34, 51-55

Horvitz HR, Herskowitz (1992) Mechanisms of asymmetric cell division: two Bs or not two Bs, that is the question, Cell 68, pp. 237–255

Huang Y (2002) Transciptional silencing in *Saccharomyces cerevisiae* and *Schizosaccharomyces pombe*. Nucl. Acids Res. 30, 1465-1482.

Kaeberlein M, Powers RW, Steffen KK, Westman EA, Hu D, Dang N, Kerr EO, Kirkland KT, Fields S, et al. (2005) Regulation of yeast replicative life span by TOR and Sch9 in response to nutrients. Science, 310:1193–1196

Kaeberlein, M.;Burtner, C.; Kennedy, BK (2007) Recent developments in aging. PloS Genet. doi: 10.1371/journal.pgen.0030084.

Kauffman SA (1969) Metabolic stability and epigenesis in randomly constructed genetic nets. Journal of Theoretical Biology, 22:437-467

Kauffman SA (1993) Origins of Order: Self-Organization and Selection in Evolution Oxford University Press.

Kennedy BK, Austriaco JrNR, Guarente L (1994) Daughter cells of Saccharomyces cerevisiae from old mothers displays a reduced life span. J. Cell Biol. 127, 1985-1993.

Kirkwood T (1981) Repair and its Evolution: Survival versus Reproduction, Chapter 7. Physiological Ecology: An Evolutionary Approach to Resource Use, Blackwell Scientific Publications, Oxford.

Kirkwood TB (2005) Understanding the odd science of aging. Cell 120: 437–447

Kirkwood TBL (1977) Evolution of ageing. Nature 270, 301–304

Kirkwood TBL (1989). DNA, mutations and aging. Mutat. Res. 219, pp. 1–7

Kirkwood TBL (1999) Time of our Lives: The Science of Human Ageing. London: Weidenfeld and Nicolson.

Kirkwood TBL, Franceschi C (1992) Is aging as complex as it would appear? Ann. NYAcad. Sci. 663, pp. 412–417

Kirkwood TBL, Holliday R (1979) The evolution of ageing and longevity. In: Proc. R. Soc. Lond., Ser. B 205, pp. 531–546

Kirkwood TBL, Rose MR (1991) ‘‘Evolution of Senescence: Late Survival Sacrificed for Reproduction.’’ Philosophical Transactions of the Royal Society of London B332 15–24.

Kitano H (2002) Computational Systems Biology Nature. 420, 206-210

Kitano H (2002) Standards for modeling Nat. Biotech. 20, 337

Kitano H (2002) Systems Biology: A Brief Overview. Science. 295, 1662-1664

Kitano H (2007) Towards a theory of biological robustness, Mol Syst Biol 3, pp. 1–7

Klipp E, Herwig R., Kowald A., Wierling C and Lehrach H (2005) Systems Biology in Practice: Concepts, Implementation and Application. Wiley-VCH, Weinheim

Klipp E, Liebermeister W, Helbig A, Kowald A & Schaber J. (2007) Systems Biology standards – the community speaks. Nature Biotechnology, 25(4), 390-391

Kowald A, Kirkwood TBL (1993) Mitochondrial mutations, cellular instability and ageing: Modeling the population dynamics of mitochondria. Mutat. Res. 295, pp. 93–103

Kowald A, Kirkwood TBL (1994) Towards a network theory of ageing: A model combining the free radical theory and the protein error theory. J. Theor. Biol. 168, pp. 75–94

Kowald A, Kirkwood TBL (1996) A network theory of ageing: the interactions of defective mitochondria, aberrant proteins, free radicals and scavengers in the ageing process. Mutat. Res. 316, pp. 209–236

Kowald A, Kirkwood TBL (1997) Network theory of ageing, Experimental Gerontology Volume 32, Issues 4-5, pp. 395-399

Le Novère, N. *et al* (2005) Minimum information requested in the annotation of biochemical models (MIRIAM). Nature Biotechnology 23:1509-1515

Leupold U (1970) Genetical methods for *Schizosaccharomyces pombe*. Methods Cell Physiol. 4, 169-177.

Levine RL (2002) Carbonyl modified proteins in cellular regulation, aging, and disease. *Free Radic Biol Med* 32: 790−796

Lin SJ, Kaeberlein M, Andalis AA, Sturtz LA, Defossez PA, Culotta VC, Fink GR, Guarente L. (2002) Calorie restriction extends *Saccharomyces cerevisiae* lifespan by increasing respiration. Nature, 418:344–348

Lindner AB, Madden R, Demarez A, Stewart EJ, Taddei F (2008) Asymmetric segregation of protein aggregates is associated with cellular aging and rejuvenation Proc. Natl. Acad. Sci. USA 105, 3076 – 3081

Mangel M (2001) Complex adaptive systems, aging and longevity, J. Theor. Biol. 213, pp. 559–571.

Martin SG, Chang F. (2005) New end take off, regulating cell polarity during the fission yeast cell cycle. Cell Cycle 4, 1046-1049.

Mata J, Nurse P (1997) Tea1 and the microtubular cytoskeleton are important for generating global special order within the fission yeast cell. Cell 89, 939-949.

McMurray MA, Gottschling DE (2003). An age-induced switch to a hyper-recombinatorial state. Science 301, 1908-1911.

McRae et al., 1982. Global sensitivity analysis-a computational implementation of the Fourier amplitude sensitivity test (FAST). Comput. Chem. Eng. v6. 15-25.

Medawar P (1957) An unsolved problem in biology. In: The Uniqueness of the Individual. Basic Books, pp. 1–27

Medvedev, ZA (1981) On the immortality of the germ cell line. Int J Dev Biol, 42, 1037-1042.

Mitchison JM, Nurse P (1985) Growth in cell length in the fission yeast *Schizosaccharomyces pombe*. J. Cell Sci. 75, 357-376.

Mortimer R, Johnston J (1959) Lifespan of Individual Yeast Cells. Nature 183:1751-1752

Nasim A, Young P, Johnson BF (1989) Molecular biology of the fission yeast. Academic Press, New York, NY

Nyström T (2002) Translational fidelity, protein oxidation, and senescence: lessons from bacteria. Aging Res Rev 1: 693−703

Nyström T. (2005) Role of oxidative carbonylation in protein quality control and senescence. EMBO J. 24:1311–131

Nyström, T (2007) A Bacterial Kind of Aging. PLoS Genet 3(12): e224

Orgel LE (1963) The maintenance of the accuracy of protein synthesis and its relevance to ageing. In: Proc. Natl. Acad. Sci. USA 49, pp. 517–521

Partridge L, Barton NH (1993) Optimality, mutation and the evolution of ageing Nature 362, 305-311.

Partridge L, Gems, D (2006) Beyond the evolutionary theory of ageing, from functional genomics to evo-gero, Trends in ecology & evolution, vol. 21, n°6, pp. 334-340

Partridge L. (2001) Evolutionary Theories of Ageing Applied to Long-lived Organisms, Experimental Gerontology 36 (2001): 641–650.

Pratt JM et al. (2002) Dynamics of protein turnover, a missing dimension in proteomics. Mol. Cell. Proteomics 1, 579-591.

Rogina, B, Helfand, SL (2004) Sir2 mediates longevity in the fly through a pathway related to calorie restriction. Proc. Natl. Acad. Sci. 101:15998-16003

Rosenberger RF (1991) Senescence and the accumulation of altered proteins. Mutat. Res. 256, pp. 255–262

Runarsson TP, Yao X (2000) Stochastic Ranking for Constrained Evolutionary Optimization IEEE Transactions on Evolutionary Computation, Vol. 4, No. 3, pp. 284-294

Rupes I, Jia Z, Young PG (1999) Ssp1 promotes actin depolymerization and is involved in stress response and new end take-off control in fission yeast. Mol. Biol. Cell 10, 1495-1510.

Shankaranarayana G, Motamedi MR, Moazed D, Grewal SI (2003) Current Biol. 13, 1240-1246

Sheldrake AR (1974) The ageing, growth and death of cells. Nature 250,381

Sinclair D (2002) Paradigms and pitfalls of yeast longevity research. Mech. Ageing Dev. 123: 857-867

Sinclair D, Guarente L (1997) Extrachromosomal rDNA circles-a cause of aging in yeast. Cell 91, 1033-1042.

Sinclair D, Mills K, Guarente L, (1998) Ageing in Saccharomyces cerevisiae, Annu. Rev. Microbiol, , 52:533-60

Soueidan H, Sherman DJ and Nikolski M (2007) *BioRica:* A multi model description and simulation system, Proceedings of the 2nd Foundations of Systems Biology in Engineering (FOSBE), pp. 279-287, Fraunhofer IRB Verlag, ISBN 978-3-8167-7436-5

Stadtman ER (1992) Protein oxidation and aging. Science 257, 1220-1224.

Stadtman, ER, Levine, RL (2000) Protein Oxidation. Ann. N.Y. Acad. Sci. 899, 191-208.

Stewart EJ, Madden R, Paul G, Taddei F (2005) Aging and death in an organism that reproduces by morphologically symmetric division. PLoS Biol 3, e45

Tissenbaum, HA, Guarente, L (2001) Increased dosage of a sir-2 gene extends lifespan in *C. elegans*. Nature, 410: 227-230

Watve M, Parab S, et al. (2006) Aging may be a conditional strategic choice and not an inevitable outcome for bacteria. Proc. Natl. Acad. Sci. USA 103, 14831-5.

Westendorp RGJ, Kirkwood TBL (1988) Human Longevity at the Cost of Reproductive Success, Nature 396: 743–746.

Westerhoff HV et al. (2008) Systems biology towards life in silico: mathematics of the control of living cells, J Math Biol.

Westerhoff HV, Palsson BO (2004) The evolution of molecular biology into systems biology, Nat Biotechnol 22, pp. 1249–1252

Woldringh CL, Fluiter K, Huls PG (1995) Production of senescent cells of *Saccharomyces cerevisiae* by centrifugal elutriation. Yeast 11, 361-369.

Wolkenhauer O (2005) Systems Biology: Dynamic Pathway Modeling

Xue H et al. (2007) A modular network model of aging, Molecular Systems Biology 3:147

You L (2004) Toward Computational Systems Biology, Cell Biochemistry and Biophysics, Volume 40, Number 2, pp. 167-184(18)

Zi Z, Klipp E (2006) SBML-PET: a Systems Biology Markup Language-based parameter estimation tool. Bioinformatics 22, 2704-2705.

Appendix A

A.1 Quantitative results of population study

a)

Type of division	Asymmetrically dividing system without retention	Asymmetrically dividing system with retention 0.875	Symmetrically dividing system without retention	Symmetrically dividing system with retention 0.875
Population size area	35310.39	13385	1022.9	1450.82

b)

Type of comparison	50-50 re 0.875 vs. 50-50 no re	25-75 re 0.875 vs. 25-75 no re		25-75 no re vs. 50-50 no re	25-75 re 0.875 vs. 50-50 re 0.875	
damage	1.8	<1.8	>1.8	All	<0.8	>0.8
Partial winners	1.56*	2.7	1.27	34.52	12.93	1.6
overall	1.42	2.64		34.52	9.2	

Table A1| Population summary. a| Total population size area for each division type. The areas are calculated using numerical integration of the functions obtained by fitting the data points from simulations using least-square method. **b| Comparisons between different types of division with or without retention are shown.** *Overall* section gives an estimate of how much is one population favorable then the other. It is simply the ratio of first and second model we compared (e.g. 1.42=1450.82/1022.9). *Partial winners* section gives the closer insight how favorable one model is to the other under different damage rates (e.g. up to the damage rate 1.8 asymmetrically dividing system with retention 0.875 is 2.7 better then the same system without retention, while for the damages higher then 1.8 system without retention is 1.27 times better). * 1.56 is comparison of population sizes (not the areas) for this particular damage rate, since this is the only point when symmetrical system without retention will overcomes same system with retention.

A.2 Quantitative results of damage partitioning

size / re	Asymmetrical division		Symmetrical division	
	25	**75**	**50d**	**50m**
0	0.25	0.75	0.5	0.5
0.125	0.21875	0.78125	0.4375	0.5625
0.25	0.1875	0.8125	0.375	0.625
0.375	0.15625	0.84375	0.3125	0.6875
0.5	0.125	0.875	0.25	0.75
0.625	0.09375	0.90625	0.1875	0.8125
0.75	0.0625	0.9375	0.125	0.875
0.875	0.03125	0.96875	0.0625	0.9375

Table A.2| Distribution of damage. Distribution of damage is not only depending of retention coefficient, but it depends on the size of the entity as well. In the table different retention coefficients and different sizes of the entity and actual distribution of damage are presented.

A.3 Carbonilation levels – simulation results

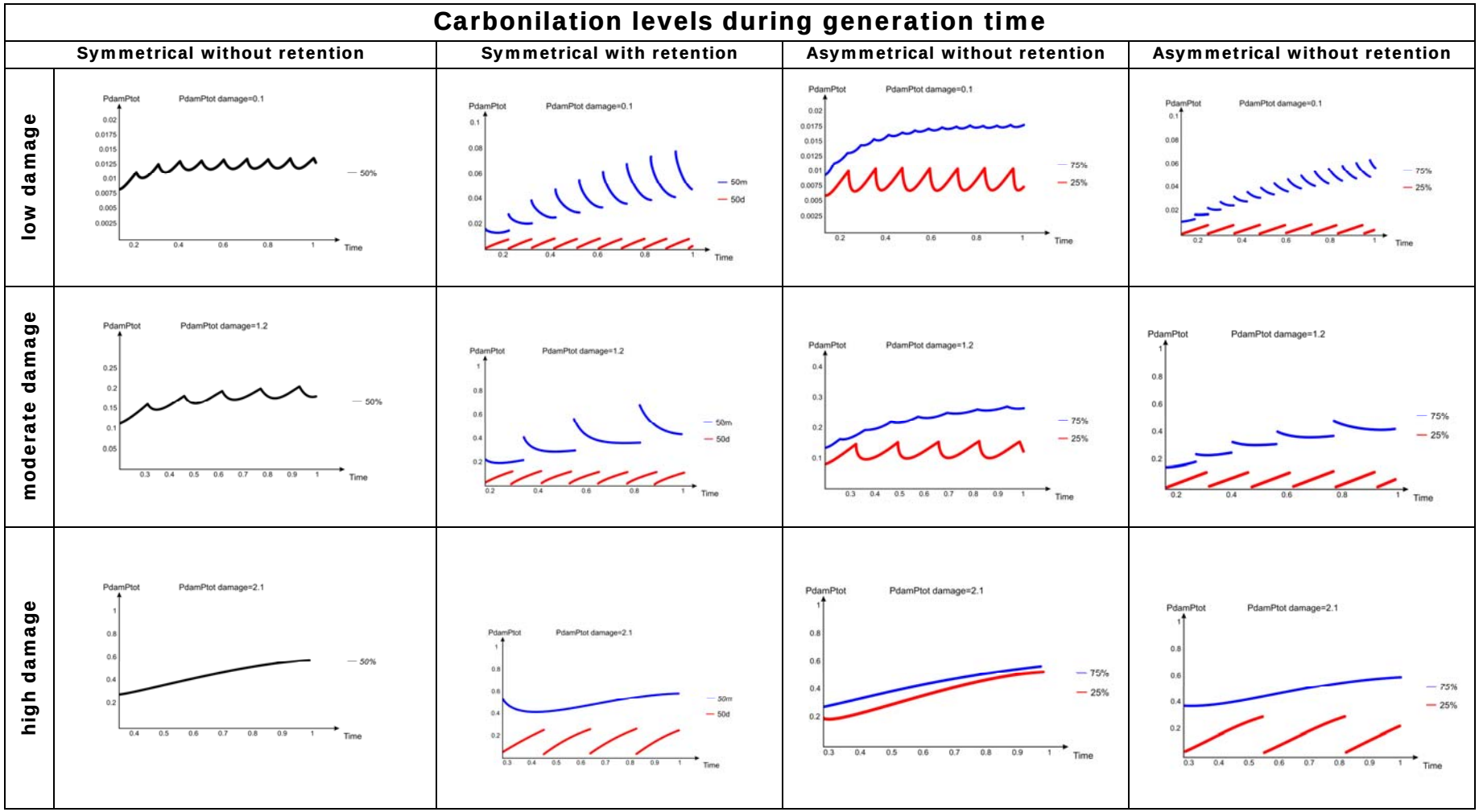

Figure A3| Carbonilation levels during generation time. Asymmetric and symmetric division, with and without damage segregation, for low, moderate and high damage rates. Mother's lineages are presented in blue, daughters in red.

Appendix B

B.1 Derivation of the equation for cell division

When constructing the equations for cell division we assumed that amounts of intact and damage proteins within the progenies and progenitors are constant before and after the division.
Also, the amounts of intact (damage) proteins are conserved within the entity (entity is defined as a mother and/or as a daughter) before and after the division.

When including the retention coefficient in the equations, the distribution of intact will depend on levels of damaged proteins, retention and size of the cell, due to the above assumptions.

1. Damaged proteins in the mother cell:

Assumption:

$$P_{dam}(1-m) \rightarrow P_{dam}(1-m)(1-re) \qquad (1)$$

$$P_{dam}m \rightarrow P_{dam}mX$$

$$\Rightarrow X = \frac{1-(1-m)(1-re)}{m}$$

Follows:

$$P_{dam}m \rightarrow P_{dam}(m+(1-m)re) \qquad (2)$$

2. Intact proteins in the daughter cell:

Assumption:

$$P_{dam}(1-m) \rightarrow P_{dam}(1-m)(1-re)$$

$$P_{int}(1-m) \rightarrow P_{int}(1-m)Y$$

$$\Rightarrow Y = 1+\frac{P_{dam}}{P_{int}}re$$

Follows:

$$P_{int}(1-m) \rightarrow P_{int}(1-m)(1+\frac{P_{dam}}{P_{int}}re) \qquad (3)$$

3. Intact proteins in the mother cell:

Assumption:

$$P_{dam} m \rightarrow P_{dam}(m + (1-m)re)$$

$$P_{int} m \rightarrow P_{int} mZ$$

$$\Rightarrow Z = 1 - \frac{P_{dam}}{P_{int}} \frac{1-m}{m} re$$

Follows:

$$P_{int} m \rightarrow P_{int} m(1 - \frac{P_{dam}}{P_{int}} \frac{1-m}{m} re) \qquad (4)$$

Where:

m - mother

$1-m$ - daughter

re - retention in the mother

$1-re$ - retention in the daughter

Finally:

From (1) and (4) follows:

$$\begin{aligned} P_{dam}(g+1) &= P_{dam}(g) \cdot s_{daughter} \cdot (1-re) \\ P_{int}(g+1) &= P_{int}(g) \cdot s_{daughter} + P_{dam}(g) \cdot s_{daughter} \cdot re \end{aligned} \qquad (5)$$

And the total amount of proteins in the cell in the next generation (P(g+1)) is simply the sum of the equations (5):

$$P(g+1) = P_{int}(g) \cdot s_{daughter} + P_{dam}(g) \cdot s_{daughter}$$

And this is the set of equations describing the cell division for the progenies and corresponds to the equations 4.6 given in this thesis.
Similarly, the equations 4.5 can be derived.

B.2 Euler's method for solving ODEs

Theorem (Euler's Method)

Euler's Method assume that $f(t,y)$ is continuous and satisfies a Lipschits condition[1] in the variable y, and consider the initial value problem:

$y' = f(t,y)$ with $y(a) = t_0 = \alpha$, over the interval $a \le t \le b$.

Euler's method uses the formulas:

$t_{k+1} = t_k + h$, and $y_{k+1} = y_k + hf(t_k, y_k)$ for $k = 0,1,2,...,m-1$

as an approximate solution to the differential equation using the discrete set of points

$$\{(t_k, y_k)\}_{k=0}^{m}$$

Error analysis for Euler's Method

When we obtained the formula $y_{k+1} = y_k + hf(t_k, y_k)$ for Euler's method, the neglected term for each step has the form $\frac{y^{(2)}(c_k)}{2}h^2$. If this was the only error at each step, then at the end of the interval $[a,b]$, after **m** steps have been made, the accumulated error would be:

$$\sum_{k=1}^{m} \frac{y^{(2)}(c_k)}{2}h^2 = m\frac{y^{(2)}(c)}{2}h^2 = \frac{hmy^{(2)}(c)}{2}h = \frac{(b-a)y^{(2)}(c)}{2}h = o(h^1)$$

[1] A function $f(x)$ satisfies the Lipschitz condition of order β at $x = 0$ if $|f(h) - f(0)| \le B|h|^{\beta}$ for all $|h| < \varepsilon$, where **B** and β are independent of $h, \beta > 0$, and α is an upper bound for all β for which a finite **B** exists.

B.3 BioRica system

System

BioRica is a high-level modeling framework integrating discrete and continuous multi-scale dynamics with the same semantic domain, offering an easy to use and computationally efficient numerical simulator.

It is in this precise sense of mixing different dynamics that BioRica models are *hybrid* following classical definitions. Moreover, BioRica models are built hierarchically. Alur et al. defined two types of hierarchy: *architectural* and *behavioral*. While BioRica admits both, in this work we are only concerned with the former. This type of hierarchy allows for both concurrency and parallel composition. Each cell is encoded by a BioRica node that has a 2-level hierarchy: a discrete controller and a continuous system. The former detrmines the distribution of proteins at division time using the discrete transition assignements (4–6) and (7–9), while the latter determines the evolution of protein quantities during one cell cycle and is realized by the equations (1–3).

More precisely, the discrete controller is encoded by a *constraint automaton* defining the discrete transitions between states. A state of a cell c^i is a tuple $\left\langle \boldsymbol{P_{int}^i, P_{dam}^i, D^i} \right\rangle$, where $\boldsymbol{P_{int}^i}$ and $\boldsymbol{P_{dam}^i}$ are protein quantities as previously defined, and $\boldsymbol{D^i}$ is a vector of integers representing the indices of every daughter of c^i. A transition between states is a tuple $\langle \boldsymbol{G, e, A} \rangle$, where e is an event, G is a guard and A is an assignment. In our case we have: for mitosis (event e), if the threshold of the cell size is attained $P_{int} = 1500$ (guard G), then create a new BioRica node c^j for the daughter of the current cell c^i, add c^j to the vector D^i, and perform the assignments (see equation 3–6) (assignments A of state variables). A second discrete event representing clonal senescence is triggered whenever $\boldsymbol{\partial P_{int} < 0}$.

The cell population is encoded by a BioRica node using the mechanism of parallel composition. This node contains the population array *Pop*, the root of the lineage tree *R*

and the parameter vector $\vec{\boldsymbol{P}}$. Since our model focuses on the division strategy, it considers the growth medium as a non limiting factor; and consequently we do not account for cell to cell interactions. This absence of interaction is directly modeled by parallel composition of independently evolving cell nodes.

Algorithm

We now describe our method for efficient simulation of the cell population model described in section 4.6.3, beginning with an overview of the general simulation schema (algorithm 1) followed by a concrete specialization for damage segregation.
The simulation schema for a given BioRica node is given by a hybrid algorithm that deals with continuous time and allows for discrete events that roll back the time according to these discrete interruptions. The time advances optimally either by the maximal stepsize defined by the adaptive integration algorith, or by discrete jumps defined by the minimal delay necessary for firing a discrete event.

As shown in algorithm 1 the simulation advances in a while loop. This loop is interrupted either if the simulation time is up, or if the test alive indicates that this node has died in the current or previous state. The node evolves continuously by calling *advance_numerical_integration*, after which we check whether any guard G of some event $\langle \boldsymbol{G,e,A} \rangle$ was satisfied. In such a case a number of updates are performed: the time is set to the firing time of e, e is stored in the trace database, the current state S is set according to the algebraic equation A, and the numerical integrator is reset to take into the account the discontinuity. The correctness of algorithm 1 is assured by the fact that no discrete event is missed. As illustrated on figure 4.5, the step size proposed by the numerical integrator guarantees that the continuous function is linear between the current time t and the maximal step size. In this way the detection of discrete events whose guards have been satisfied in this interval is reduced to computing the *first intersection*. It is the event e with the smallest firing time that is retained for the next discrete transition. After this transition the numerical integrator has to restart from the point defined by A.

Implementation

The software architecture of the BioRica platform consists of three main parts: the compiler, the simulator and the interface. The compiler transforms the textual description of the model given in the BioRica modeling language or an SBML file into a set of C++ classes, each of them corresponding to a distinct Bio-Rica component. These classes are linked at compile time with a static BioRica library that runs the simulation. This library provides methods for multithreaded multi-scale hybrid simulation, by using numerical integrators of the GSL library that interacts with a discrete event solver. The simulator generated in native code accepts command line arguments setting the simulation-specific (maximal time, random seed etc.) and model-specific parameters. Simulation results are stored in a relational database. In the context of the damage segregation model, the requirement is to be able to store lineages trees. This implies a serialization step that flattens the tree topology in order to represent it as a vector of couples of cells ids. These couples are directly encoded as a database table, in relation with a table storing the model-specific parameters. The latter enables fixed point detection, as well as provides the possibility to pause and restart batches of simulation at any time and at any node during the exploration of the model. A set of python scripts performs simulation trace analysis. In particular, generation of graphical output using the *graphviz* package, interactive visualization with the Tulip software, and statistical analysis with *R* and *Mathematica*. Notice that since we put no restrictions on the guards of the events of a node, more than one guard can be satisfied in the same state and at the same time. If the system is in one of those non deterministic states, the simulation algorithm needs to decide which of those concurrent events will be scheduled. To this end, the discrete controller part optionally describes the probability of an event relatively to other concurrent events. A more advanced description can even contain probability distribution on the events duration, thus enabling stochastic race conditions between concurrent events.

Appendix C

C.1 Carbonilation assay of yeast proteins using slot blots

Derivatisation of protein samples:

- Dissolve 1 µg protein sample in PEB* for a total volume of 5 µl (if necessary, dilute the original sample, as to have a suitable amount of liquid to add).
- Add: 5 µl SDS 10-12% (w/v) + 10 µl 1x DNPH (hood!)
- Vortex and spin down.
- Let reaction proceed for 15 min at RT.
- Block reaction by adding 7,5 µl of neutralizing solution (*Oxyblot kit, Intergen*) and mix immediately, so that color turns uniformly from yellow to red.
- Add sterile water up to a final volume of 80 µl, vortex and spin down (keep samples on ice).

Dot blotting:

- Cut out a piece of PVDF membrane and wet it briefly in transfer buffer**.
- Cut out 3-5 sheets of Watman 3 paper of the same size and wet them briefly in the same transfer buffer.
- Insert the paper in the slot blotter, cover with the membrane and tighten well the top lid on the blotter.
- Attach the blotter to the vacuum pump, check that the transfer buffer is passing through.
- Load duplicates of 35 µl each of the protein samples in the single slots.
- When blotting is complete, remove the vacuum tube and open the blotter.
- Wash the membrane in PBS-Tween + Milk powder, to block the proteins, and leave it shaking for ~ 40 min (you can also leave the membrane incubating ON at 4°C.
- Wash the membrane 2-3 x with a small amount of PBS-Tween, to remove the milk.
- Add a solution of the 1st antibody (50 ml PBS-Tween + 333 µl Rabbit-Anti DNP).
- Incubate shaking for 1h: 30 min, RT.

- Wash the membrane 3x 10 min in PBS-Tween.
- Add a solution of the 2nd antibody (50 ml PBS-Tween + 166 µl Goat-Rabbit-Anti DNP).
- Incubate shaking for 30 min.
- Wash 2x 5 min + 3x 10 min in PBS-Tween.
- Add Horseradish Peroxidase solution (5 ml Luminogen reagent + 125 µl reagent B, *ECL-PLUS, Amersham Pharmacia*).
- Incubate 5 min, RT, shaking and then insert between two overheads and visualize.

*PEB (Protein Extraction Buffere) : - 10% glycerol
- 2mM EDTA pH 8
- 1mM Pefablock or Phenantroline or PMSF as protease inhibitors;

** Transfer Buffer : - 100 ml 10X Transfer Buffer
- 200 ml MetOH / EtOH
- 700 ml dd-water

10X Transfer Buffer:
- 30 g Tris base
- 144 g Glycine
- 10 g SDS
- dd-water to a final vol of 1 l

C.2 Separation of Mother and Daughter Cells

Old mother cells were obtained by centrifugal elutriation (38) by using a J-20 XP centrifuge equipped with a JE 5.0 rotor (Beckman Coulter, Fullerton, CA). To enrich the culture for old cells, two successive rounds of elutriation were performed, allowing for over night growth in between. Cells were subsequently resuspended in PBS and loaded in a 40-ml separation chamber at 32 ml/min and312–385 X *g*; old cells were elutriated at 90 ml/min and 35–62 X *g*. The cells thus obtained were grown again for one generation and subjected to a last round of elutriation at the same settings to separate the mothers from their daughters. Separation of young mother and daughter cells was achieved by loading exponentially growing cultures in a 5-ml separation chamber and by using a cutoff of 10

ml/min at 728 X g (daughters) or 20 ml/min at 385 X *g* (mothers). The efficiency of every sorting was confirmed by Calcofluor White (Sigma, St. Louis, MO) staining and bud scar counting.

C.3 *S.pombe* protocol

Strains

All strains used in this study were isogenic or derivatives of the 972h$^-$ wild type and were kindly provided by Per Sunnerhagen at the CMB, Göteborg University. The *sir2Δ* and *tea1Δ* mutants were derived from strain sp286 (ade6-210 ura4-D18 leu1-32 h$^+$) and had the gene of interest replaced by a KanMX4 cassette.

Immunofluorescence

Cells were grown to OD_{600}=0,7 in YES medium (1% yeast extract, 3% glucose), washed and resuspended in 50 ml PBS. They were then synchronized by centrifugal elutriation using a JE5 rotor (Beckman-Coulter) so that those with a length of <9 μm were collected at 1800 rpm and 45 ml/min. The cells collected were resuspended in YES and allowed to grow at 30°C. Aliquots were taken at different times hereafter and stained with calcofluor white to determine the septum and birth scar(s) location. *In situ* preparation and detection of carbonyls was carried out as described previously with some modifications. Approximately 30-40 cells were analyzed for each sample.

Treatment with Latrunculin A (Wako) and Benomyl (Fluka) was carried out as previously described, and co-staining with DAPI and Fluorescein-Phalloidin (Mol. Probes) was performed in accordance with previous protocols.

Life span analysis

Wild type cells were placed on a plate and allowed to divide once at which point the sibling devoid of birth scars was kept, while its sister was discarded. This “virgin” sib was then followed for 9 successive generations, by removing the “scar-free” sister sibs generated at every division. At this point both siblings were isolated: the one with the

greater number of birth scars and roundest appearance was defined as the “old” sib; whereas its more regularly-shaped “scar-free” counterpart was defined as the “new” sib. The replicative fates of these two sibs were then followed independently and their generation times and number of divisions were recorded.

Acknowledgements

Now it is time to write the page that would probably have the highest access☺. That's how it goes with thesis – people first read your acknowledgement page and then they might go on.

Before I start thanking people that made my PhD life one extremely nice experience, I would first have to thank some unknown people in Brussels for making great decision of investing some of the EU money to science. My PhD journey was financed by Marie Curie grant - Early Stage Training in Systems Biology (more officially and according to strict EU regulations – MEST-CT2004-514169).

On this great journey first person I met was my supervisor **Edda Klipp** at Max Planck Institute for Molecular Genetics in Berlin. Thank you Edda, for giving me the opportunity to be a part of your group and to work on this truly fantastic topic. I would also, like to thank you for teaching me how research should be done, for your guidance, for always being there when I needed you and most importantly for giving me freedom to do things my way. I admire you for everything you did and still doing and I am very privileged to be your student.
In my group in Berlin, I would like to thank to some special guys: **Jannis** – the programming master – thanx for all the scripts you made for me and for all the calls to Arcor and Berliner Sparkasse. **Zhike** – thanx for counting my virtual cells, for all the movie suggestions, for being happy and positive person. **Matteo** – the pasta master – thanx for extremely delicious and endless Italian meals, for vivid discussions we had – I will definitely miss this.

My thesis would not be complete without the help of Ageing master – **Thomas Nyström** at Göteborg Univeristy. Thank you Thomas for giving me the opportunity to work along side biologist. Replacing my laptop with the pipette and elutriator was quite an experience. You helped me to get deeper understanding for yeast, to open my mind and not to become pure theoretician. It was a great honor to be a part of your group.
There are many people in famous TN-group that taught me to love and understand yeast and many other important things.
Laurence – you are one of the first persons I met in my Göteborg life. Totally unexpectedly it turn out that we are going to share scientific life and enjoy many fikas together. Thanx for enjoyable life-important discussions and all respect for finishing 2 marathons! **Malin** – thanx for having understanding for each and everyone, your passion for science is incredible as well as cycling very fast on Hisingenrunt. We have to do it again next year. **Bertil** - thanx for sharing my love for Abercrombie and Fitch and the cute guys in front of their shops. **Antonio** – thanx for bringing light and Spanish spirit in our lives, and lab-pets Ricky Martin and Justin T. Pity we had to share you with micromanipulator for many hours. **Veronica** – my great room mate. It is difficult to imagine sharing the office with some else. Regular laughing sessions and every day chats made days goes faster. Thanx for being so positive person and don't worry you will

become master of elutriation very soon! **Lisa M** – sporty Lisa, wise and realistic; it was a pleasure having you around. **Nika** – you taught me how to pipette, how to make perfect slot-blot and how to enjoy perfect cup of espresso. It was a real joy working and discussing science and life issues with you. **Mikael** – bird watcher – a fantastic one, walking and eating very fast. I am still not convinced that you are just watching birds…just kidding☺. **Martin** – you can start talking about any topic, you brought a new wave into this group. **Beidong** – table tennis and shooting master, it was nice having you around. **Örjan** – a fighter and a collector of nice bikes. **Lisa L** – only person respecting the rules and actually wearing the coat in the lab. **Dani** – food is my passion guy; you are a great friend and wonderful person. It was so nice having you in the group past months. **Åsa** – it is good to have you back in this lab. **Anne** – thanx for all delicious Thanksgiving turkeys and games we had with you.

I would also have to thank to 'fantastic three' from Bordeaux: **Hayssam, David** and **Macha**. It was great doing science and having famous Bordeaux wine and French cheese with you guys.

This whole work would not be possible without constant love, care and support from my parents and my brother **Ivan**. I consider myself extremely lucky for having great and supporting family. Thank you for everything. Žile, it is hard to find the words that will show how much I love you and how much I miss not have you closer to me. You are everything and much more then anyone can wish for a brother.

And finally I have to say huge thank you for the best guy in the whole world, the one that went trough so many things with me and the one that understands me entirely – my **Nikola**. **Pilence – VKMN!**

Ehrenwörtliche Erklärung

Hiermit erkläre ich, dass ich diese Arbeit selbstständig verfasst und keine anderen als die angegebenen Hilfsmittel und Quellen verwendet habe.

Marija Cvijovic

Berlin, July 2008